Response to Reviewers' comments, observations, and actions taken thereof while revising the Manuscript ID: nhess-2022-66 Titled "**Site Characterization vis-à-vis Probabilistic Seismic Hazard and Disaster Potential Modelling in the Himalayan and Sub-Himalayan Tectonic Ensemble from Kashmir Himalaya to Northeast India at the backdrop of the updated Seismic Hazard of the Indian Subcontinent**" by Nath et al.

Response to the comments and observations of Anonymous Reviewer#2

Reviewer#2: General introduction: The novelty of your work is not completely clear from introduction. What is the additional value of your work to the existing literature? It should appear that this is not only an application; otherwise I don't see it suitable for this journal. Then, I recommend to update the novelty section of the work.

Authors' Response:

The Authors feel inspired by the words of appreciation and encouragement made by the Reviewer. The novelty of the work has been described in point-wise form below:

1. The Probabilistic Seismic Hazard formulation for both 10% and 2% probability of exceedance in 50 years amounting to 475 and 2475 years of return periods respectively for the Indian subcontinent have been implemented in a rigorous Logic Tree Framework consisting of the followings:

(a) Consideration of 172 polygonal as well as 3216 major tectectonic seismogenic sources defined through juxtaposition of active tectonic, seismicity and homogeneous declustered earthquake catalogue, the moment tensor solutions and faults and lineaments extracted through Remote sensing and GIS database.

(b) Consideration of multiple threshold magnitudes viz. M_w 3.5, 4.5 and 5.5 as ascertained from the complete and homogeneous declustered earthquake catalogue for 1900-2018 consisting of 64,153 main seismic events.

(c) Inclusion of depth wise variation of seismic activity rates for both the polygonal and tectonic seismogenic sources using smoothening seismicity (Frankel, 1995) for the depth ranges of 0-25km, 25-70km, 70-180km and 180-300km.

(d) Region-specific depth wise maximum earthquake prognosis from the sub-catalogues extracted from the main homogenous declustered catalogue of Nath et al. (2017).

(e) Selection of hordes of Ground Motion Prediction Equations (GMPEs) taken from all the local-specific researches totaling to about 197 of which there had been 68 Next Generation Spectral Attenuation models (NGAs) developed by Nath (2017) and Nath et al. (2021) as a part of the present research whose ranks and weights have been determined using Log Likelihood (LLH) calculations following Scherbaum et al. (2009).

(f) Usages of both the aleatory and epistemic uncertainties associated with magnitude, rupture distance and GMPEs/ NGA for all the depth wise seismogenic sources in all the tectonic territories.

2. The Socio-economic Risk Map of India is generated by integrating vulnerability exposures viz. Population Density, Building Density, Landuse/ landcover extracted from Census (2011) and Remote Sensing imagery viz. Sentinel-2, Landsat-8 and LISS-IV with IBC-compliant surface-consistent Probabilistic Seismic Hazard through an Analytic Hierarchy Process and expert judgement for the entire Indian territory.

3. An enriched database containing a huge volume of geophysical, geotechnical, geological, geomorphological and topography data has been used to towards seismic site classification and its characterization of entire ensemble from Kashmir Himalaya to Northeast India. Geology, Geomorphology, Slope and Landform are used for establishing a regional- specific empirical relation through a nonlinearly regressed 5th order polynomial equation to estimate the effective shear wave velocity (V_s^{30}) for characterizing the region into various Site classes based on NEHRP (BSSC, 2003), FEMA (2000) and Sun et al. (2018) nomenclature. Around 3000 data points have been used for the nonlinear regression analysis, out of which 80% (Training) data are considered for establishing the empirical relationship and remaining 20% (Testing) are used for the validation purposes. From the correlation between geotechnical and regional dataset, it is observed that most of the data set are lying within the 70% confidence bound and nearly follow 1:1 correspondence line as is also reported by Nath et al (2021).

We have also used the lithology-specific and depth-dependent empirical relations between SPT-N and V_s for the alluvial plain region in which lithological units have been classified into sixteen categories by Nath et al (2021) according to their grain size, plasticity index and presence or absence of decomposed wood etc. as (i) Top Soil, (ii) Sand, (iii) Sandy Silt (iv) Silty Clay with Decomposed Wood, (v) Silty Clay with Mica, Sand and/or Kankar, (vi) Clay with Decomposed Wood, (vii) Silty Sand with Mica and/or Clay (vii) Silty Clay with rusty Silty Spots, (ix) Sand with Silt and Clay, (x) Silty Sand with Mica and Kankar, (xi) Bluish/Yellowish grey Silt, (xii) Silt, (xiii) Sand and (xiv) Fine Sand with Gravel (xv) Clayey Silt and (xvi) All Soils.

4. Seismic Site Characterization has been carried out for the entire ensemble from Kashmir Himalaya to Northeast India in terms of absolute site amplification factor, spectral site amplification factor, predominant frequency and generic site amplification spectra. Surface-consistent Probabilistic Seismic Hazard assessment is done through convolution of the bedrock level hazard with estimated site amplification factors as has been presented along with design response spectra at both bedrock and surface levels for many important cities indicating an appreciable enhancement in the existing design values.

5. SELENA-based urban structural impact assessment has been carried out for the first time for a few Capital-Spiritual-Commercial Cities such as Srinagar, Chandigarh, Gurugram, Kanpur, Asansol, Chittagong, Thimphu, Shillong, Imphal, Itanagar and Kathmandu for the surface-consistent probabilistic seismic hazard for 10% probability of exceedance in 50 years. Seismic damageability functions have been derived for the three seismogenic tectonic territories viz. West-Northwest Himalaya, North-central Himalaya and Northeast India along with the countries of Nepal and Bhutan for three most prevalent building types seen across the regions i.e. Adobe (A1), Unreinforced Masonry (URM) and Reinforced Concrete (RC)-type buildings. SELENA generated hybrid predicted and scenario combined damage states have been demarcated based on simulated damage states for different earthquake scenarios and surface-consistent Probabilistic Seismic Hazard.

Thus, this work presents a unique benchmark regional-local hybrid seismic hazard-disaster model for pre-disaster preparedness in the form of updated urban by-laws and post-disaster rehabilitation and future disaster management for the ensemble.

Reviewer#2: General introduction: The introduction should be more direct to the focus of the work. A specific section on the collected data could be added. I suggest to shorten it, by moving the data to their sections.

Authors' Response: The observation has been noted and the Introduction part will be modified in the revised manuscript.

Reviewer#2: General introduction: The literature is quite incomplete with respect to the fact that the ground shaking levels recorded at adjacent buildings are going to reveal significant spatial correlation.

Goda K, Hong HP (2008) Spatial correlation of peak ground motions and response spectra. Bull Seismol Soc Am 98(1):354–365

Sokolov V, Wenzel F (2011) Influence of spatial correlation of strong ground motion on uncertainty in earthquake loss estimation. Earthq Eng Struct Dyn 40(9):993–1009.

Park J, Bazzurro P, Baker JW (2007) Modeling spatial correlation of ground motion intensity measures for regional seismic hazard and portfolio loss estimation. Applications of statistics and probability in civil engineering. Taylor & Francis Group, London, pp 1–8

Miano, A., Jalayer, F., Forte, G., & Santo, A. (2020). Empirical fragility assessment using conditional GMPE-based ground shaking fields: Application to damage data for 2016 Amatrice Earthquake. Bulletin of Earthquake Engineering, 18(15), 6629-6659.

Authors' Response: The followings have already been incorporated in the electronic supplement of the revised manuscript. However, if the Reviewer so desires that the same need be part of the main manuscript we will do the needful while revising the manuscript and shift the same from the electronic supplement to the main body of the manuscript.

"For establishing the accuracy of these NGA models worked out for the eleven tectonic provinces we compared the PGA values of the predicted NGA model considering Atkinson and Boore (2006), with the recorded and simulated ones in the corresponding seismogenic zones and observed a satisfactory agreement amongst all of them. Representative plots of PGA vs. fault distance for six seismogenic tectonic blocks *viz*. Kashmir Himalaya, Northwest India, Indo-Gangetic Foredeep region, Bengal Basin, Darjeeling-Sikkim Himalaya and Northeast India have been depicted in **Figure S3** in the electronic supplement. Few representative plots of PSA at 0.2sec, 0.3sec and 1.0sec derived from both NGA models and the simulation with respect to fault distance have been also shown in **Figure S4** in the electronic supplement for Kashmir Himalaya, Northwest India, Indo-Gangetic Foredeep region and Northeast India (Shillong Zone) source zones.

(a) Kashmir Himalaya Tectonic Province:

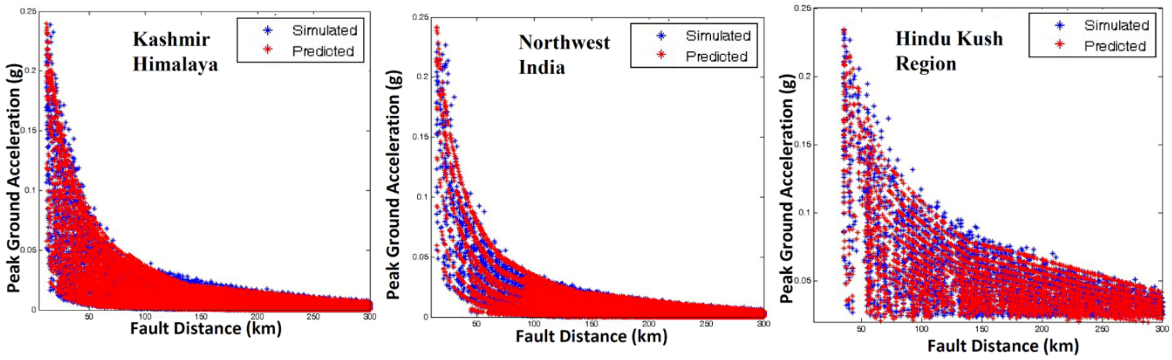

(b) Northwest India Tectonic Province:

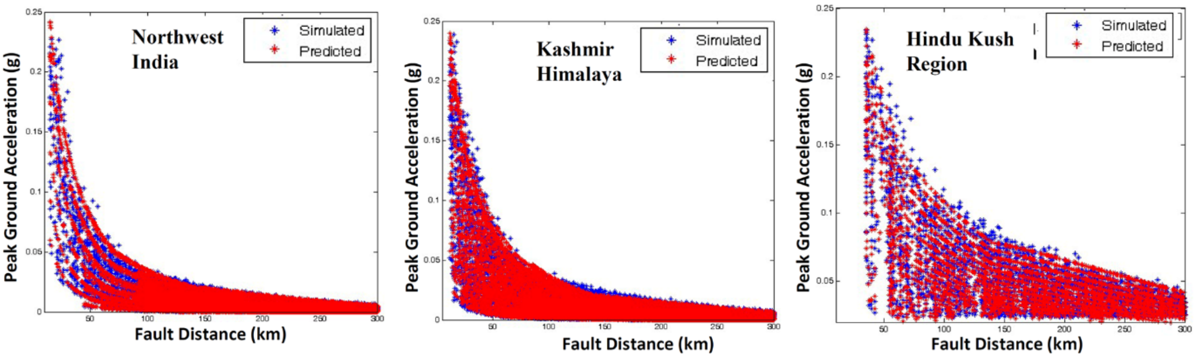

(c) Indo-Gangetic Foredeep Tectonic Province:

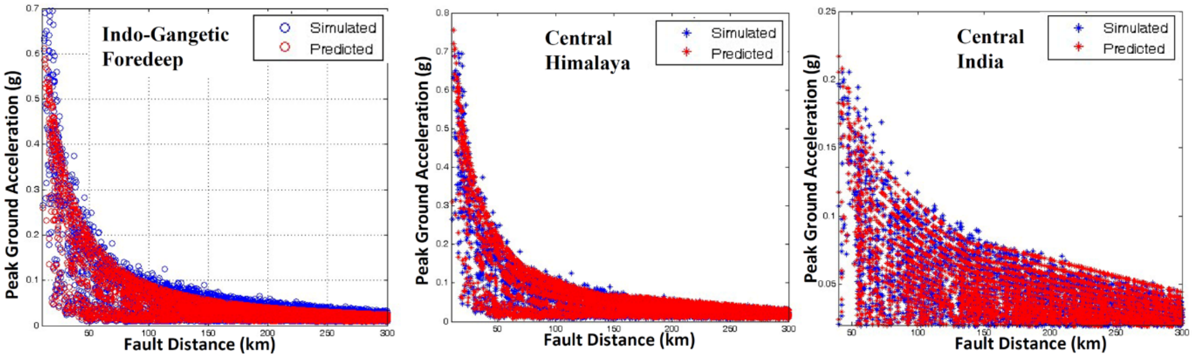

(d) Bengal Basin Tectonic Province:

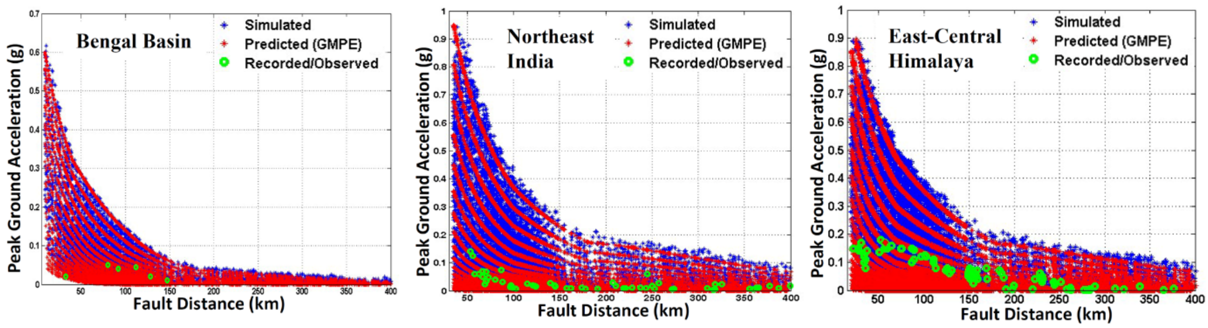

(**e**) Darjeeling-Sikkim Himalaya Tectonic Province:

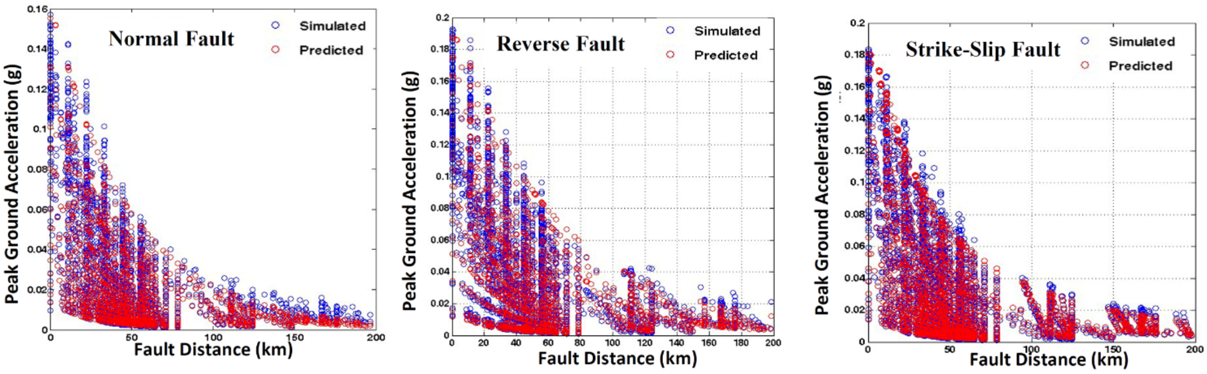

(**f**) Northeast India Tectonic Province:

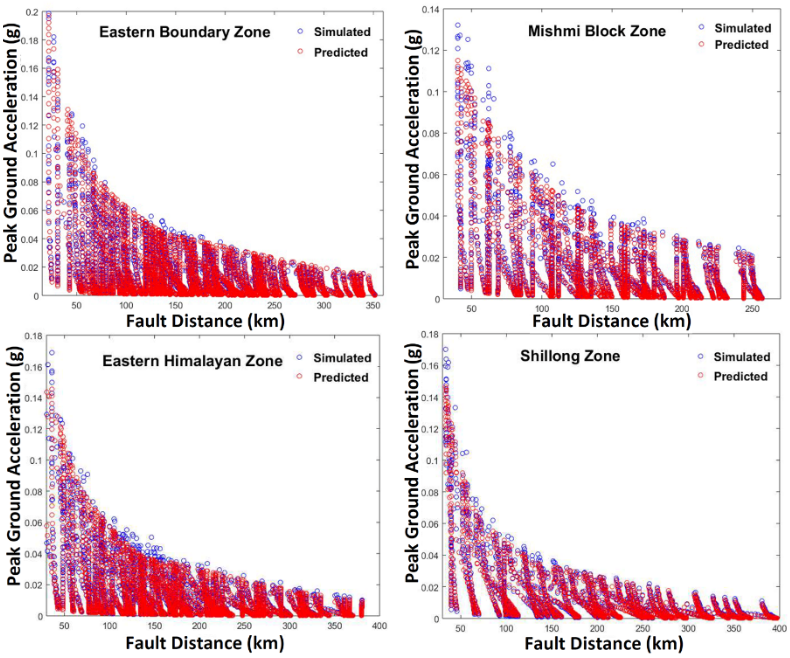

Figure S3. Peak Ground Acceleration (PGA) with respect to fault distance for corresponding seismogenic sources for the seismogenic tectonic provinces of (a) Kashmir Himalaya, (b) Northwest India, (c) Indo-Gangetic Foredeep (Nath et al., 2019), (d) Bengal Basin (Nath et al., 2014), (e) Darjeeling-Sikkim Himalaya and (f) Northeast India. The blue dots represent the simulated PGA; the red dots represent the estimated PGA from predicted NGA models of Atkinson and Boore (2006) and the green dots represent the recorded PGA for each seismogenic sources.

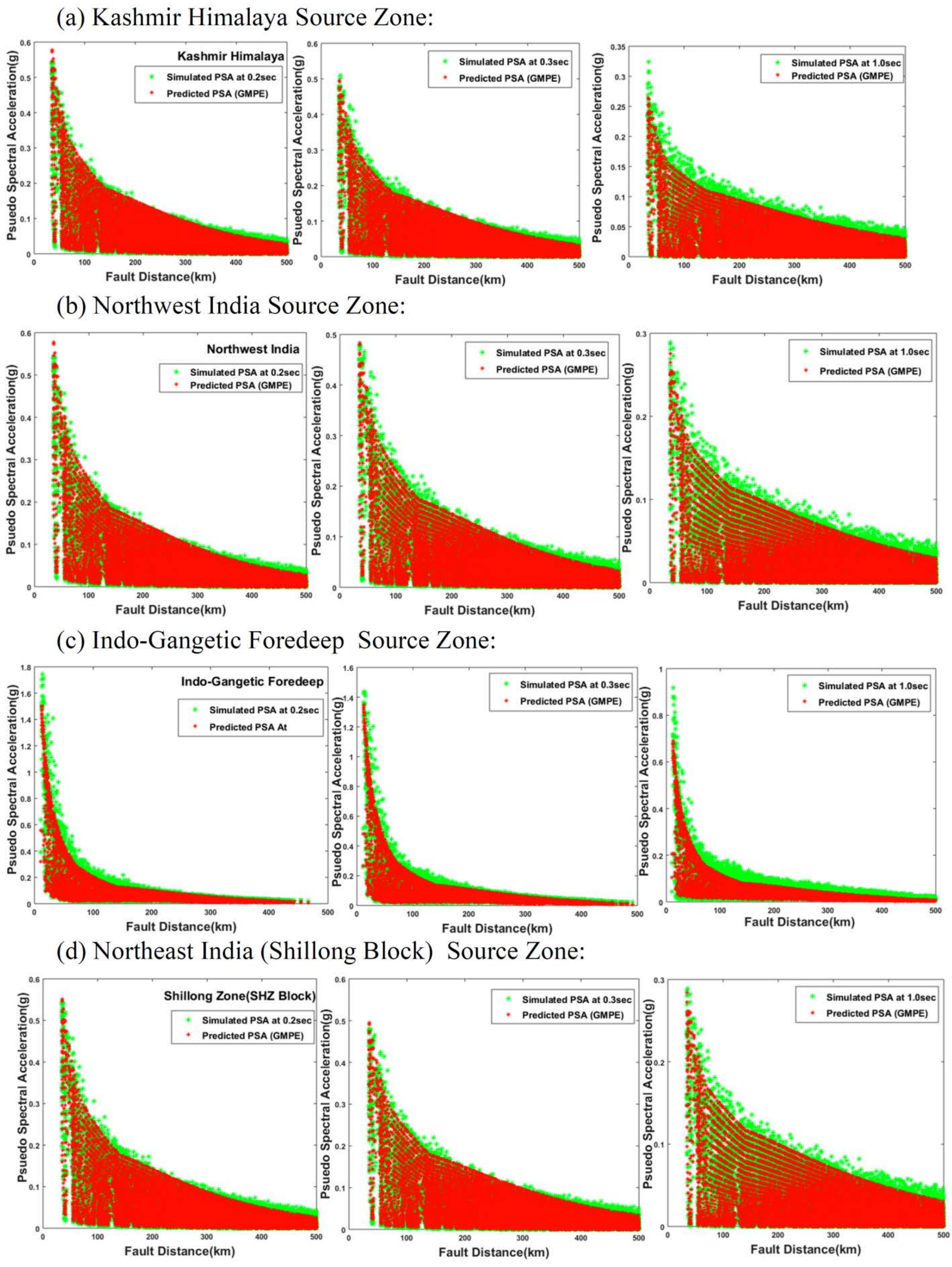

Figure S4. Representative Pseudo Spectral Acceleration (PSA) at 0.2sec (left), 0.3sec (middle) and 1.0sec (right) with respect to fault distance for seismogenic source zones of (a) Kashmir Himalaya, (b) Northwest India, (c) Indo-Gangetic Foredeep and (d) Northeast India (Shillong Zone). The green dots represent the simulated PSA and the red dots represent the estimated PSA from predicted NGA models of Atkinson and Boore (2006) for each seismogenic sources.

These predicted NGA models have further been validated using a PGA and PSA residuals assessment following the formulation,

$$residual = \log_{10}\left(\frac{Y_{os}}{Y_p}\right) \tag{S1}$$

Where, Y_{os} is the recorded and simulated PGA/PSA, Y_p is the estimated PGA/PSA from the empirical attenuation relations. Residual plots for PGA as a function of fault distance for predicted NGA models of Atkinson and Boore (2006) for all the seismogenic sources corresponding to six tectonic provinces are shown in **Figure S5** in the electronic supplement. It is evident that the residuals have a zero mean and are uncorrelated with respect to fault distance. Apparently residual analysis of PGA and PSA of the NGA models predicted in the present investigation are found to be unbiased with respect to both the magnitude & the fault distance and hence can be used along with other already available Ground Motion Prediction Equations (GMPEs) for the region and also those available for similar tectonic setup in a logic tree framework for seismic hazard assessment.

(a) Kashmir Himalaya Tectonic Province:

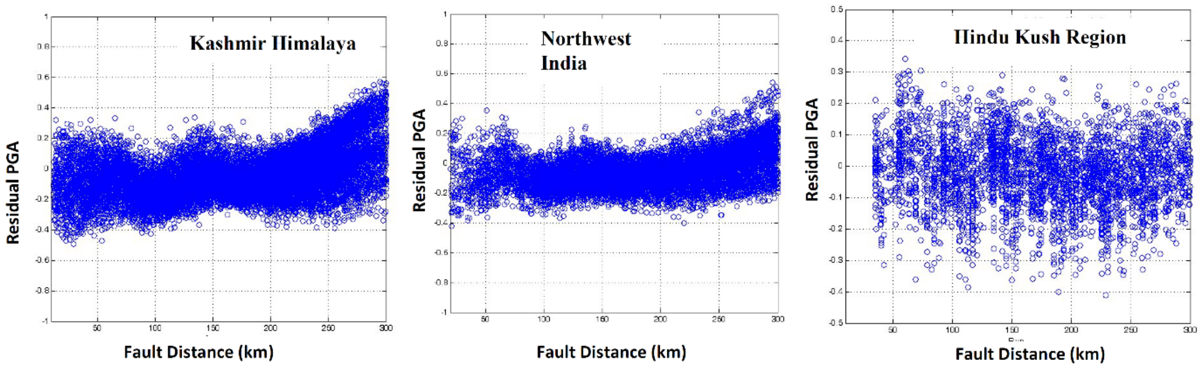

(b) Northwest India Tectonic Province:

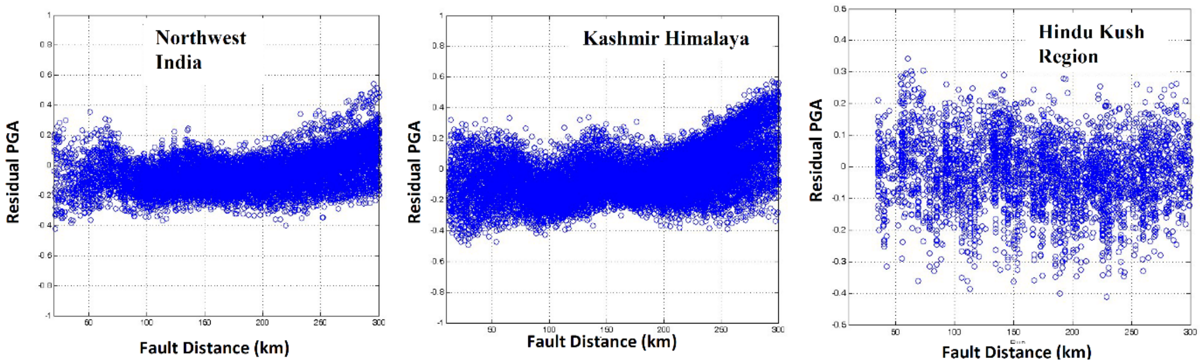

(c) Indo-Gangetic Foredeep Tectonic Province:

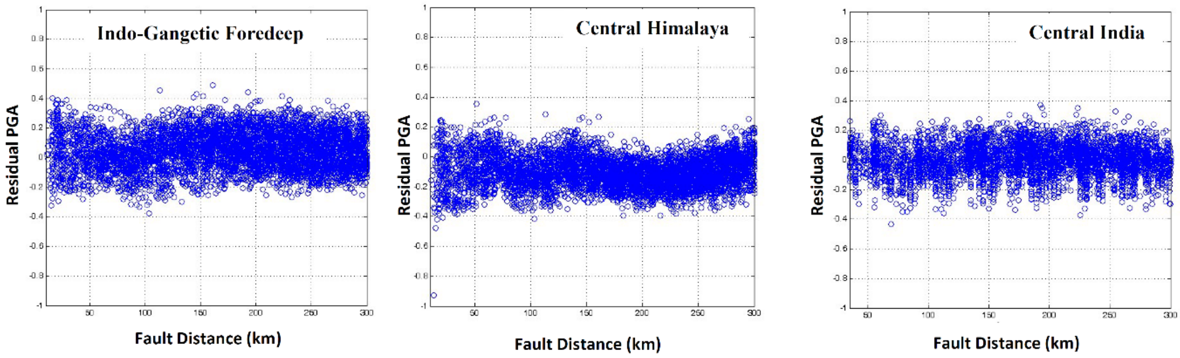

(d) Bengal Basin Tectonic Province:

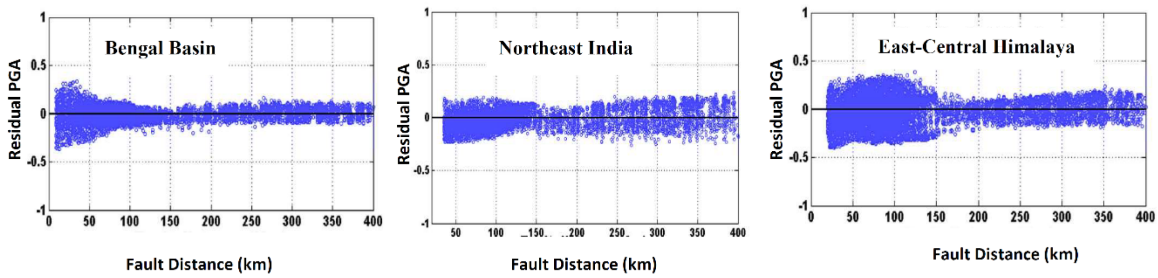

(e) Darjeeling-Sikkim Himalaya Tectonic Province:

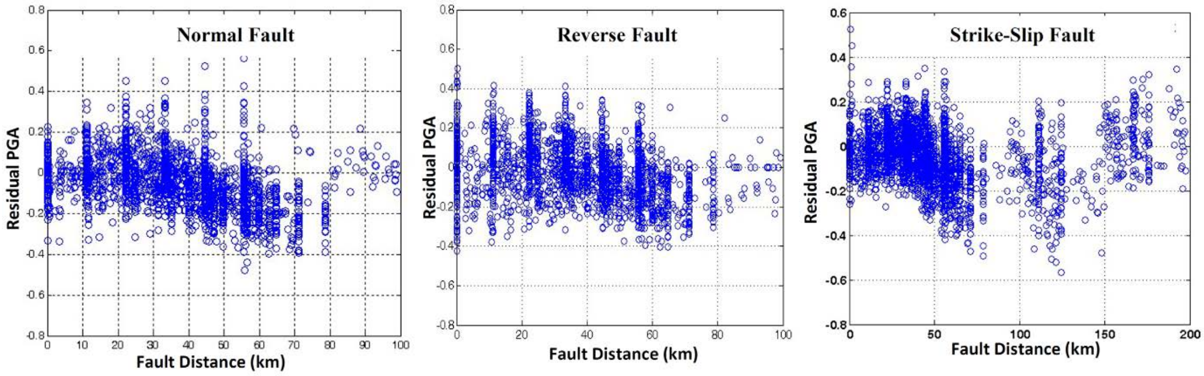

(f) Northeast India Tectonic Province:

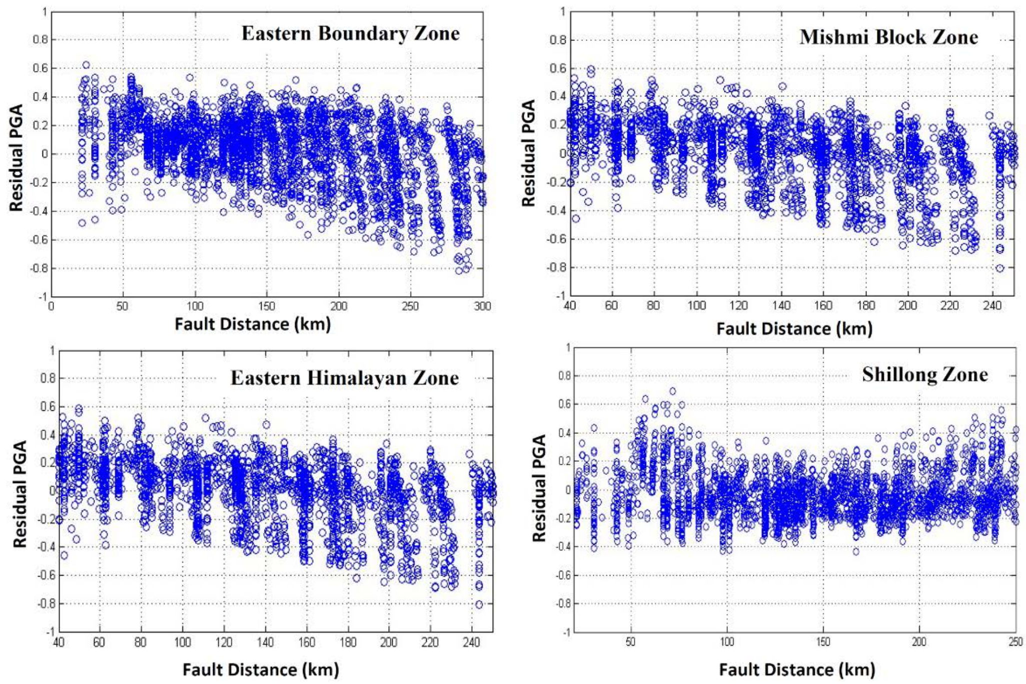

Figure S5. Residuals of PGA with respect to fault distance for corresponding seismogenic sources for the seismogenic tectonic provinces of (a) Kashmir Himalaya, (b) Northwest India, (c) Indo-Gangetic Foredeep (Nath et al., 2019), (d) Bengal Basin (Nath et al., 2014), (e) Darjeeling-Sikkim Himalaya and (f) Northeast India (Nath et al., 2009) considering NGA model of Atkinson and Boore (2006).

Apart from our own Prediction equations worked out as a part of this investigation we also incorporated some regional and global prediction models based on the suitability test performed on each such model for the estimation of seismic hazard of the region. We adopted 197 Ground Motion Prediction Equations (GMPEs) including 68 NGAs as given in **Table S1** in the electronic supplement for hazard computations in eleven blocks. The coefficients of GMPEs already available for the regions as worked out by other researchers in this territory have been adopted from their original publications. Appropriate selection and ranking of Ground Motion Prediction Equations (GMPEs) is critical for a successful logic-tree implementation in the probabilistic seismic hazard analysis. Quantitative suitability assessment, referred to as 'efficacy test', of a GMPE for a particular region is decisive in providing a ranking order for a suite of GMPEs towards the best possible selection. These are performed based on the efficacy test of the GMPEs towards suitability of adaptation in comparison with the observed earthquakes in the region. Towards this, we employed an information-theoretic approach proposed by Scherbaum et al. (2009). The efficacy test makes use of average sample log-likelihood (LLH) computation for the purpose of ranking. The LLH is computed as,

$$LLH = -\frac{1}{N}\sum_{i=1}^{N}\log_2(g(x_i)) \tag{S2}$$

Where, x_i represents the observed data for $i = 1, ... N$. The parameter N is the total number of events and $g(x_i)$ is the likelihood that model g has produced the observation x_i. In this case, g is the probability density function given by a GMPE to predict the observation produced by an earthquake with magnitude M at a site i that is located at a distance R from the source.

Table S1. Selected Ground Motion Prediction Equations for PSHA of the Indian Peninsula predominantly comprising of eleven Seismogenic Tectonic Provinces shown in **Figure 2** in the manuscript.

Seismogenic Tectonic Province	Seismogenic Sources	Global/Regional Ground Motion Prediction Equations (GMPEs)	Next Generation Attenuation (NGA) Models
Bengal Basin including Bangladesh	East-Central Himalaya	Sharma et al. (2009); Toro (2002); Campbell and Bozorgnia (2008)	Nath (2017); Campbell and Bozorgnia (2003); Atkinson and Boore (2006)
	Bengal Basin	Raghukanth and Iyengar (2007); Toro (2002)	Nath et al. (2014); Maiti et al. (2017); Nath (2017); Campbell and Bozorgnia (2003); Atkinson and Boore (2006)
	Northeast India	Youngs et al. (1997); Campbell and Bozorgnia (2008); Nath et al. (2012) (Shallow and Deep crust)	Nath et al. (2009); Nath et al. (2012); Nath (2017); Campbell and Bozorgnia (2003); Atkinson and Boore (2006)
Indo-Gangetic Foredeep	Indo-Gangetic Foredeep	NDMA (2010); Abrahamson and Silva (2008); Raghukanth and Kavitha (2014)	Nath et al. (2019); Nath (2017); Campbell and Bozorgnia (2003); Atkinson and Boore (2006)
	Central Himalaya	Anbazhagan et al. (2013); Sharma et al. (2009); Chiou and Youngs (2008)	Nath (2017); Campbell and Bozorgnia (2003); Atkinson and Boore (2006)
	Central India	Raghukanth and Iyengar (2007); Toro (2002); NDMA (2010)	Nath (2017); Campbell and Bozorgnia (2003); Atkinson and Boore (2006)
	Central India	Raghukanth and Iyengar (2007); Toro (2002); NDMA (2010)	Nath (2017); Campbell and Bozorgnia (2003); Atkinson and Boore (2006)

Koyna-Warna Region	Kutch Region	Boore and Atkinson (2008); Sadigh et al. (1997); NDMA (2010)	Nath (2017); Campbell and Bozorgnia (2003); Atkinson and Boore (2006)
	Koyna-Warna Region	Raghukanth and Iyengar (2007); Sharma et al. (2009); Youngs et al. (1997)	Nath (2017); Campbell and Bozorgnia (2003); Atkinson and Boore (2006)
Western Ghat Region	Western Ghat Region	Raghukanth and Iyengar (2007); NDMA (2010); Hwang and Huo (1997)	Nath (2017); Campbell and Bozorgnia (2003); Atkinson and Boore (2006)
	Eastern Ghat Region	Raghukanth and Iyengar (2007); NDMA (2010); Hwang and Huo (1997)	Nath (2017); Campbell and Bozorgnia (2003); Atkinson and Boore (2006)
	Koyna-Warna Region	Raghukanth and Iyengar (2007); Sharma et al. (2009); Youngs et al. (1997)	Nath (2017); Campbell and Bozorgnia (2003); Atkinson and Boore (2006)
Eastern Ghat Region	Western Ghat Region	Raghukanth and Iyengar (2007); NDMA (2010); Hwang and Huo (1997)	Nath (2017); Campbell and Bozorgnia (2003); Atkinson and Boore (2006)
	Eastern Ghat Region	Raghukanth and Iyengar (2007); NDMA (2010); Hwang and Huo (1997)	Nath (2017); Campbell and Bozorgnia (2003); Atkinson and Boore (2006)
	Koyna-Warna Region	Raghukanth and Iyengar (2007); Sharma et al. (2009); Youngs et al. (1997)	Nath (2017); Campbell and Bozorgnia (2003); Atkinson and Boore (2006)
Northwest India including Nepal Himalaya	Kashmir Himalaya	Anbazhagan et al. (2013); Raghukanth and Kavitha (2014); Sharma et al. (2012)	Nath (2017); Campbell and Bozorgnia (2003); Atkinson and Boore (2006)
	Northwest India	Anbazhagan et al. (2013); Raghukanth and Kavitha (2014); Harbindu et al. (2014)	Nath (2017); Campbell and Bozorgnia (2003); Atkinson and Boore (2006)
	Hindu Kush Region	Anbazhagan et al. (2013); Raghukanth and Kavitha (2014); Youngs et al. (1997)	Nath (2017); Campbell and Bozorgnia (2003); Atkinson and Boore (2006)
Darjeeling-Sikkim Himalaya	Normal Fault	Anbazhagan et al. (2013); Raghukanth and Kavitha (2014); NDMA (2010); Toro (2002); Akkar and Bommer (2010); Lin and Lee (2008); Chiou and Youngs (2008); Zhao et al. (2006); Atkinson and Boore (2006);	Adhikari and Nath (2016); Nath (2017); Campbell and Bozorgnia (2003); Atkinson and Boore (2006)

		Abrahamson and Silva (2008); Campbell and Bozorgnia (2008)	
	Reverse Fault	Anbazhagan et al. (2013); Raghukanth and Kavitha (2014); NDMA (2010); Toro (2002); Akkar and Bommer (2010); Lin and Lee (2008); Chiou and Youngs (2008); Zhao et al. (2006); Atkinson and Boore (2006); Abrahamson and Silva (2008); Campbell and Bozorgnia (2008); Sharma et al. (2009); Nath et al. (2012)	Adhikari and Nath (2016); Nath (2017); Campbell and Bozorgnia (2003); Atkinson and Boore (2006)
	Strike-slip Fault	Anbazhagan et al. (2013); Raghukanth and Kavitha (2014); NDMA (2010); Toro (2002); Akkar and Bommer (2010); Lin and Lee (2008); Chiou and Youngs (2008); Zhao et al. (2006); Atkinson and Boore (2006); Abrahamson and Silva (2008); Campbell and Bozorgnia (2008); Sharma et al. (2009); Nath et al. (2012)	Adhikari and Nath (2016); Nath (2017); Campbell and Bozorgnia (2003); Atkinson and Boore (2006)
Northeast India including Bhutan Himalaya	Eastern Himalayan Zone (EHZ)	Anbazhagan et al. (2013); Nath et al. (2012); Toro (2002)	Nath (2017); Campbell and Bozorgnia (2003); Atkinson and Boore (2006)
	Mishmi Block Zone (MBZ)	Nath et al. (2012); Youngs et al. (1997); Gupta (2010)	Nath (2017); Campbell and Bozorgnia (2003); Atkinson and Boore (2006)
	Eastern Boundary Zone (EBZ)	Singh et al. (2016); Gupta (2010); Youngs et al. (1997)	Nath (2017); Campbell and Bozorgnia (2003); Atkinson and Boore (2006)
	Shillong Zone (SHZ)	Nath et al. (2012); Youngs et al. (1997); Singh et al. (2016)	Nath et al. (2009); Nath et al. (2012); Nath (2017); Campbell and Bozorgnia (2003); Atkinson and Boore (2006)
Central India	Central India	Raghukanth and Iyengar (2007); Toro (2002); NDMA (2010)	Nath (2017); Campbell and Bozorgnia (2003); Atkinson and Boore (2006)
	Kutch Region	Boore and Atkinson (2008); Sadigh et al. (1997); NDMA (2010)	Nath (2017); Campbell and Bozorgnia (2003); Atkinson and Boore (2006)

	Koyna-Warna Regiom	Raghukanth and Iyengar (2007); Sharma et al. (2009); Youngs et al. (1997)	Nath (2017); Campbell and Bozorgnia (2003); Atkinson and Boore (2006)
Kutch Region	Central India	Raghukanth and Iyengar (2007); Toro (2002); NDMA (2010)	Nath (2017); Campbell and Bozorgnia (2003); Atkinson and Boore (2006)
	Kutch Region	Boore and Atkinson (2008); Sadigh et al. (1997); NDMA (2010)	Nath (2017); Campbell and Bozorgnia (2003); Atkinson and Boore (2006)
	Koyna-Warna Region	Raghukanth and Iyengar (2007); Sharma et al. (2009); Youngs et al. (1997)	Nath (2017); Campbell and Bozorgnia (2003); Atkinson and Boore (2006)
Kashmir Himalaya	Kashmir Himalaya	Anbazhagan et al. (2013); Raghukanth and Kavitha (2014); Sharma et al. (2012)	Nath (2017); Campbell and Bozorgnia (2003); Atkinson and Boore (2006)
	Northwest India	Anbazhagan et al. (2013); Raghukanth and Kavitha (2014); Harbindu et al. (2014)	Nath (2017); Campbell and Bozorgnia (2003); Atkinson and Boore (2006)
	Hindu Kush Region	Anbazhagan et al. (2013); Raghukanth and Kavitha (2014); Youngs et al. (1997)	Nath (2017); Campbell and Bozorgnia (2003); Atkinson and Boore (2006)

The smaller the value of LLH, the higher is the ranking index of the GMPE. The ranking analyses were carried out using macroseismic intensity data (Martin and Szeliga, 2010) and the PGA–European Macroseismic Scale (EMS, Grünthal, 1998) relation at rock sites as given in Nath and Thingbaijam (2011). **Figure S6** in the electronic supplement presents the intensity as a function of distance for the indicated earthquakes derived from the ground motion prediction equations. The individual normalized weights of each GMPE have been derived by preparing a pair-wise comparison matrix (Saaty, 1980). The ranking analysis has been performed based on LLH values along with the weight assigned to each GMPE for the corresponding seismogenic sources in all the Tectonic Provinces. Representative weights and ranks assignment to respective GMPEs based on the average LLH ranking in the corresponding seismogenic source zones for six tectonic provinces of the ensemble have been presented in **Tables S2-S7** in the electronic supplement**.** A sample pair-wise comparison matrix for the GMPEs used in Northwest India source zone and their normalized weights has been given in **Table S8** in the electronic supplement.

(a) Kashmir Himalaya Tectonic Province:

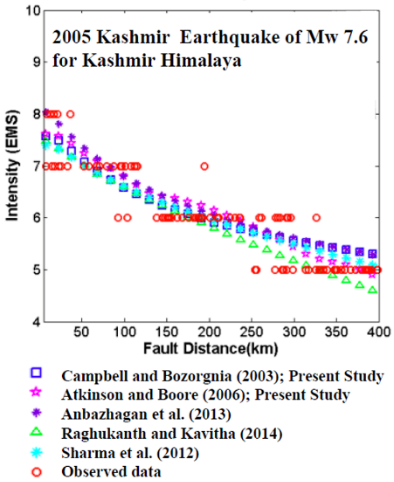

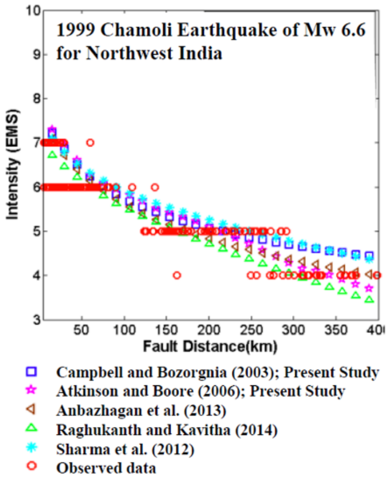

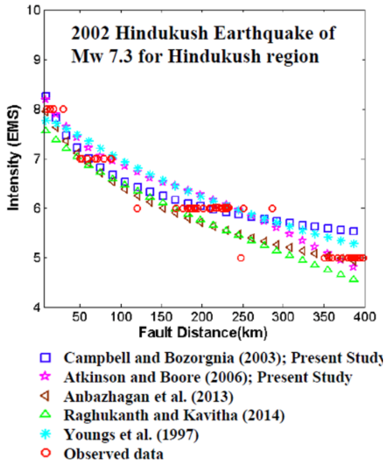

(b) Northwest India Tectonic Province:

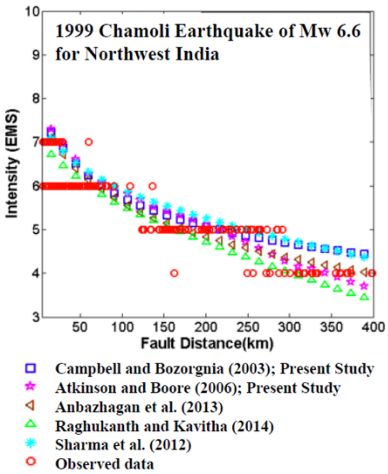

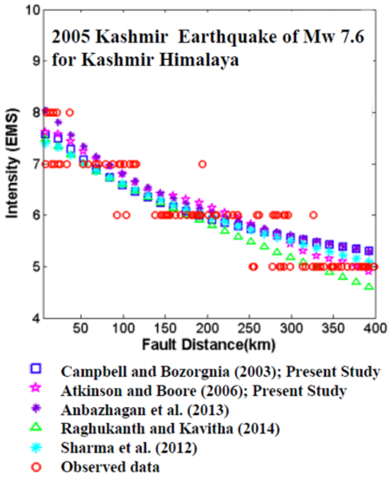

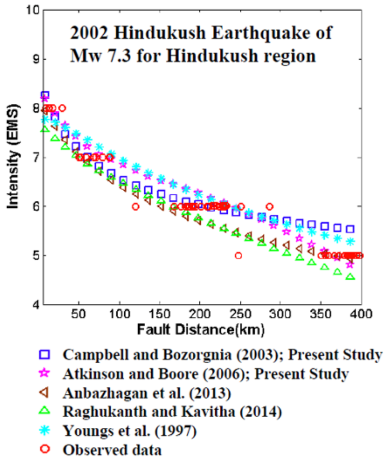

(c) Indo-Gangetic Foredeep Tectonic Province:

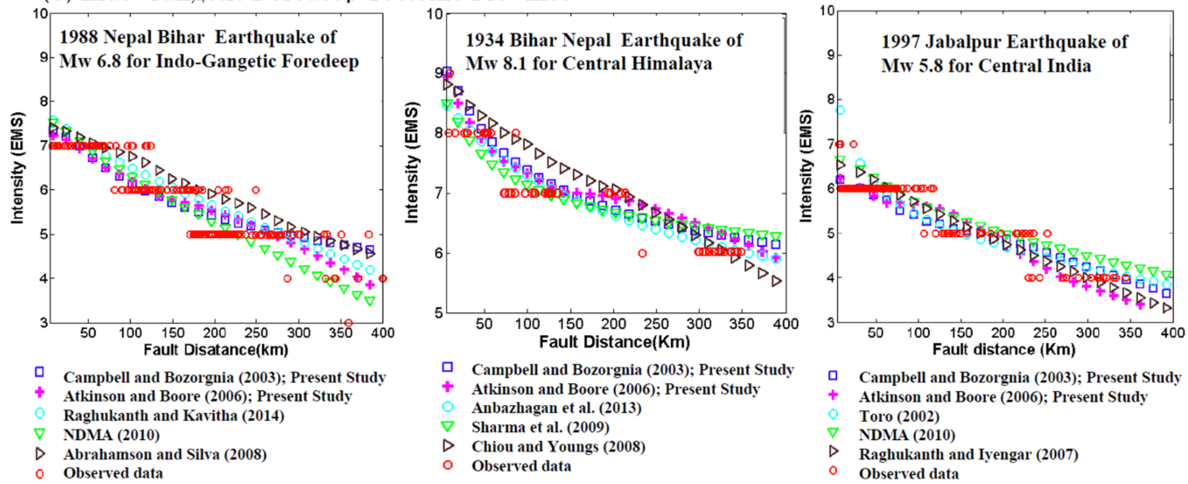

(d) Bengal Basin Tectonic Province:

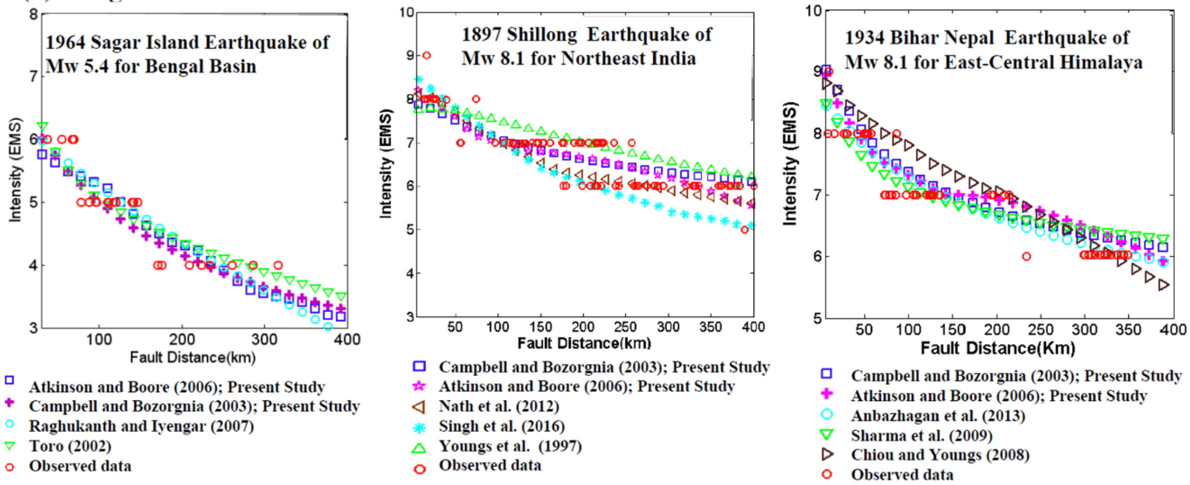

(e) Darjeeling-Sikkim Himalaya Tectonic Province:

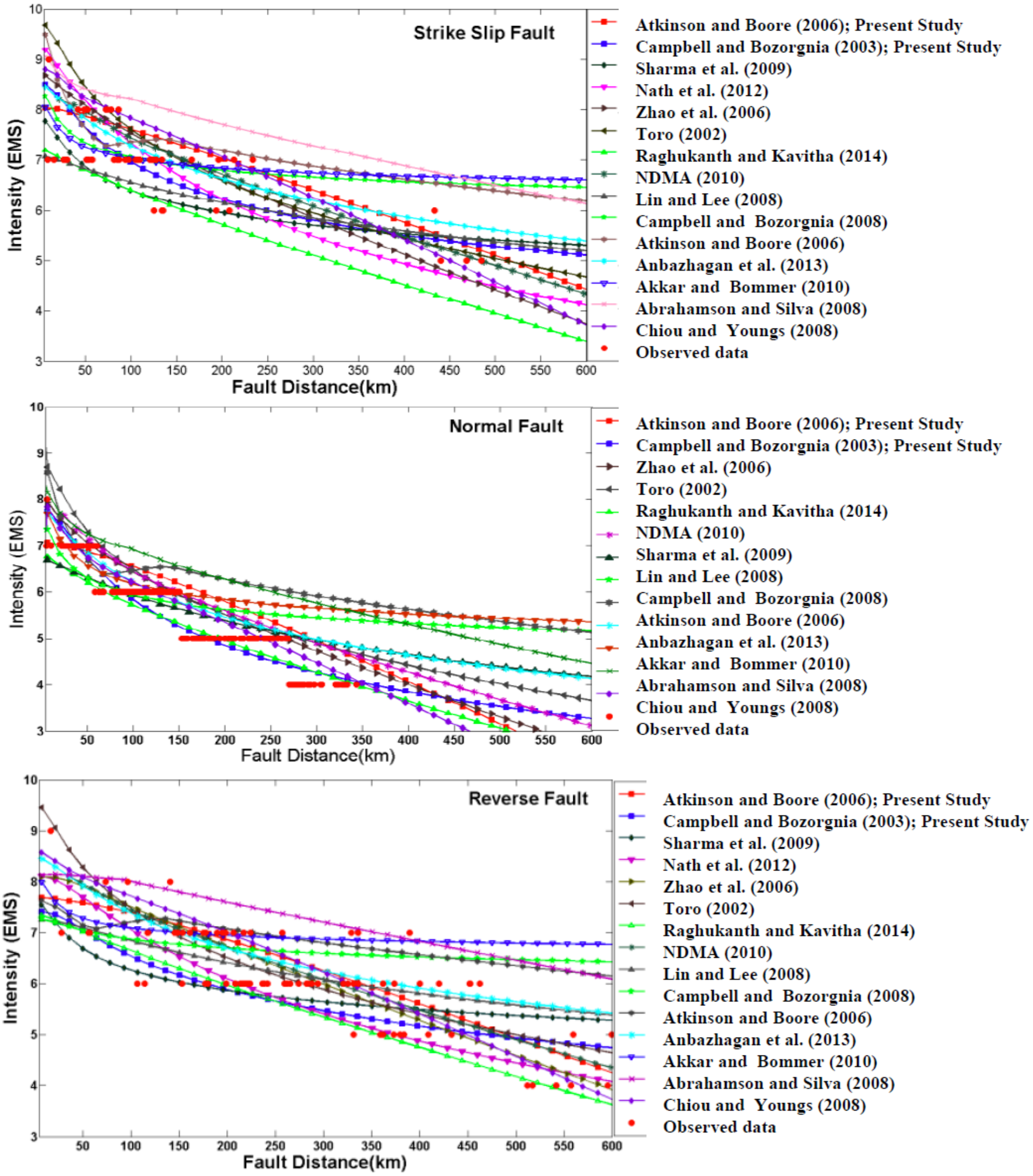

(f) Northeast India Tectonic Province:

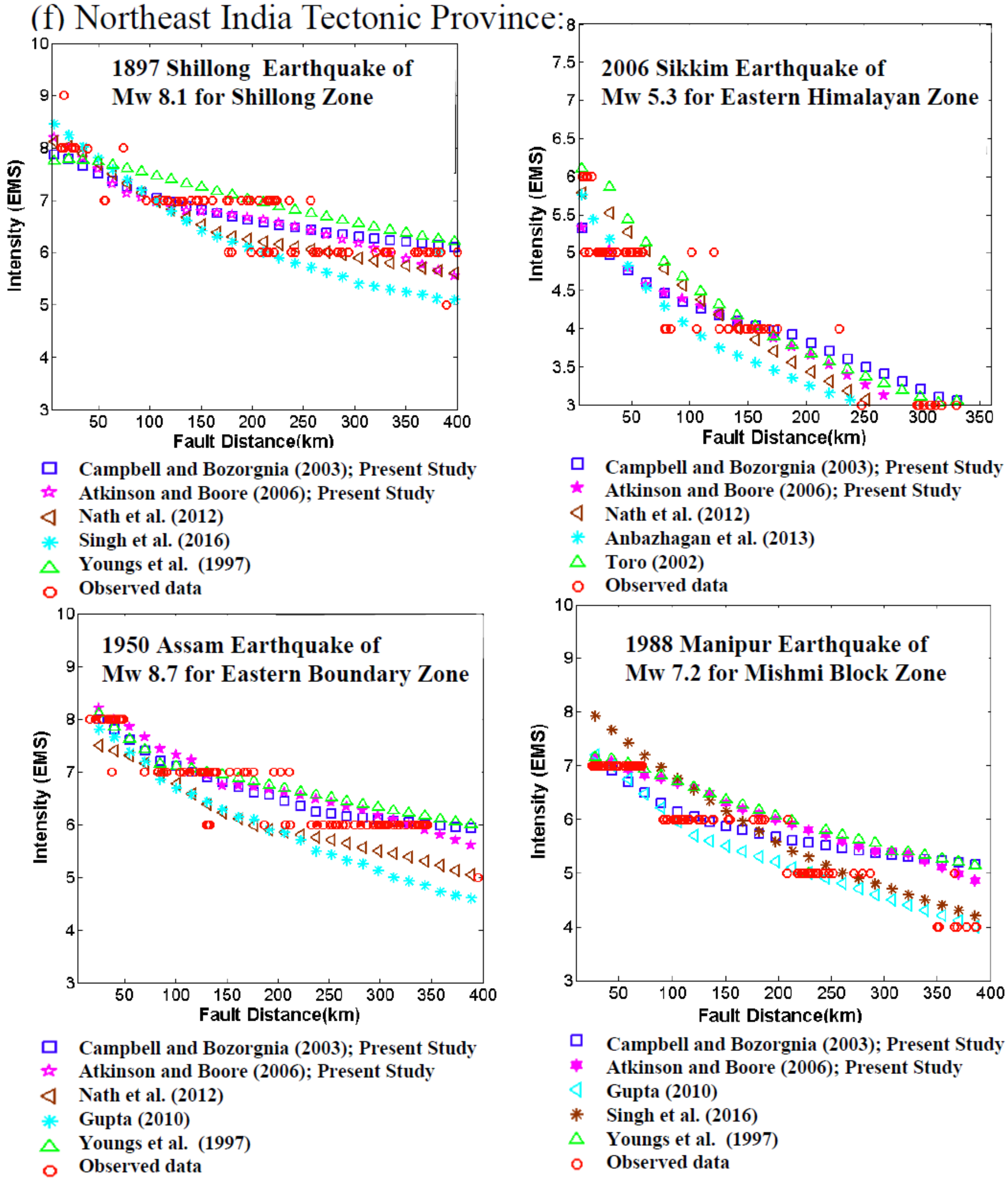

Figure S6. The intensity as a function of fault distance for the indicated earthquakes derived from the Ground Motion Prediction Equations for suitability testing of GMPEs for the seismogenic tectonic provinces of (a) Kashmir Himalaya, (b) Northwest India, (c) Indo-Gangetic Foredeep (Nath et al., 2019), (d) Bengal Basin (Nath et al., 2014; Maiti et. al, 2017), (e) Darjeeling-Sikkim Himalaya and (f) Northeast India.

Table S2. The weights and ranks assigned to respective GMPEs based on the average LLH ranking in the three seismogenic source zones for Kashmir Himalaya Tectonic Province

Kashmir Himalaya Seismogenic Source regime			
Model	LLH	Rank	Weight
Campbell and Bozorgnia (2003); Present Study	2.1279	5	0.33
Atkinson and Boore (2006); Present Study	2.1408	4	0.27
Sharma et al. (2012)	2.1505	3	0.20
Anbazhagan et al. (2013)	2.2669	2	0.13
Raghukanth and Kavitha (2014)	2.4501	1	0.07
Northwest India Seismogenic Source regime			
Model	LLH	Rank	Weight
Campbell and Bozorgnia (2003); Present Study	2.1020	5	0.33
Atkinson and Boore (2006); Present Study	2.1599	4	0.27
Harbindu et al. (2014)	2.2276	3	0.20
Anbazhagan et al. (2013)	2.2561	2	0.13
Raghukanth and Kavitha (2014)	2.2733	1	0.07
Hindu Kush Seismogenic Source regime			
Model	LLH	Rank	Weight
Campbell and Bozorgnia (2003); Present Study	2.2503	5	0.33
Atkinson and Boore (2006); Present Study	2.2648	4	0.27
Anbazhagan et al. (2013)	2.2791	3	0.20
Raghukanth and Kavitha (2014)	2.4293	2	0.13
Youngs et al. (1997)	2.6283	1	0.07

Table S3. The weights and ranks assigned to respective GMPEs based on the average LLH ranking in the three seismogenic source zones for Northwest India Tectonic Province

Kashmir Himalaya Seismogenic Source regime			
Model	LLH	Rank	Weight
Campbell and Bozorgnia (2003); Present Study	2.1279	5	0.33
Atkinson and Boore (2006); Present Study	2.1408	4	0.27
Sharma et al. (2012)	2.1505	3	0.20
Anbazhagan et al. (2013)	2.2669	2	0.13
Raghukanth and Kavitha (2014)	2.4501	1	0.07
Northwest India Seismogenic Source regime			
Model	LLH	Rank	Weight
Campbell and Bozorgnia (2003); Present Study	2.1020	5	0.33
Atkinson and Boore (2006); Present Study	2.1599	4	0.27

Harbindu et al. (2014)	2.2276	3	0.20
Anbazhagan et al. (2013)	2.2561	2	0.13
Raghukanth and Kavitha (2014)	2.2733	1	0.07
Hindu Kush Seismogenic Source regime			
Model	LLH	Rank	Weight
Campbell and Bozorgnia (2003); Present Study	2.2503	5	0.33
Atkinson and Boore (2006); Present Study	2.2648	4	0.27
Anbazhagan et al. (2013)	2.2791	3	0.20
Raghukanth and Kavitha (2014)	2.4293	2	0.13
Youngs et al. (1997)	2.6283	1	0.07

Table S4. The weights and ranks assigned to respective GMPEs based on the average LLH ranking in the three seismogenic source zones for Indo-Gangetic Foredeep Tectonic Province

Indo-GangeticForedeep Seismogenic Source			
Model	LLH	Rank	Weight
Campbell and Bozorgnia (2003); Present Study	2.144	5	0.33
Atkinson and Boore (2006); Present Study	2.346	4	0.27
NDMA (2010)	2.386	3	0.20
Abrahamson and Silva (2008)	2.510	2	0.13
Raghukanth and Kavitha (2014)	2.511	1	0.07
Central Himalaya Seismogenic Source			
Model	LLH	Rank	Weight
Campbell and Bozorgnia (2003); Present Study	2.482	5	0.33
Atkinson and Boore (2006); Present Study	2.546	4	0.27
Sharma et al. (2009)	2.552	3	0.20
Anbazhagan et al. (2013)	2.577	2	0.13
Chiou and Youngs (2008)	2.892	1	0.07
Central India Seismogenic Source			
Model	LLH	Rank	Weight
Campbell and Bozorgnia (2003); Present Study	2.201	5	0.33
Atkinson and Boore (2006); Present Study	2.219	4	0.27
Toro (2002)	2.225	3	0.20
NDMA (2010)	2.303	2	0.13
Raghukanth and Iyengar (2007)	2.389	1	0.07

Table S5. The weights and ranks assigned to respective GMPEs based on the average LLH ranking in the three seismogenic source zones for Bengal Basin Tectonic Province

Bengal Basin Seismogenic Source regime			
Model	LLH	Rank	Weight
Campbell and Bozorgnia (2003); Present Study	2.169	4	0.4
Atkinson and Boore (2006); Present Study	2.189	3	0.3
Raghukanth and Iyengar (2007)	2.368	2	0.2
Toro (2002)	2.397	1	0.1
Northeast India Seismogenic Source regime			
Model	LLH	Rank	Weight
Campbell and Bozorgnia (2003); Present Study	2.306	5	0.33
Atkinson and Boore (2006); Present Study	2.331	4	0.27
Nath et al. (2012)	2.370	3	0.20
Campbell and Bozorgnia (2008)	2.545	2	0.13
Youngs et al. (1997)	2.670	1	0.07
East-Central Himalaya Seismogenic Source regime			
Model	LLH	Rank	Weight
Campbell and Bozorgnia (2003); Present Study	2.264	5	0.33
Atkinson and Boore (2006); Present Study	2.296	4	0.27
Toro (2002)	2.371	3	0.20
Sharma et al. (2009)	2.412	2	0.13
Campbell and Bozorgnia (2008)	2.712	1	0.07

Table S6. The weights and ranks assigned to respective GMPEs based on the average LLH ranking in the three seismogenic source zones for Darjeeling-Sikkim Himalaya Tectonic Province

Strike-Slip Fault			
Model	LLH	Rank	Weight
Campbell and Bozorgnia (2003); Present Study	2.325	15	0.125
Atkinson and Boore (2006); Present Study	2.357	14	0.117
Anbazhagan et al. (2013)	2.363	13	0.108
Atkinson and Boore (2006)	2.401	12	0.100
Sharma et al. (2009)	2.421	11	0.092
Nath et al. (2012)	2.436	10	0.083
Akkar and Bommer (2010)	2.434	9	0.075
NDMA (2010)	2.441	8	0.067
Raghukanth and Kavitha (2014)	2.476	7	0.058
Lin and Lee (2008)	2.483	6	0.050
Toro (2002)	2.552	5	0.042
Campbell and Bozorgnia (2008)	2.592	4	0.033
Abrahamson and Silva (2008)	2.652	3	0.025

Chiou and Youngs (2008)	2.742	2	0.017
Zhao et al. (2006)	2.987	1	0.008
Reverse Fault			
Model	LLH	Rank	Weight
Campbell and Bozorgnia (2003); Present Study	2.222	15	0.125
Atkinson and Boore (2006); Present Study	2.285	14	0.117
Anbazhagan et al. (2013)	2.345	13	0.108
Raghukanth and Kavitha (2014)	2.389	12	0.100
NDMA (2010)	2.405	11	0.092
Nath et al. (2012)	2.495	10	0.083
Toro (2002)	2.496	9	0.075
Lin and Lee (2008)	2.497	8	0.067
Atkinson and Boore (2006)	2.504	7	0.058
Sharma et al. (2009)	2.536	6	0.050
Akkar and Bommer (2010)	2.636	5	0.042
Chiou and Youngs (2008)	2.657	4	0.033
Abrahamson and Silva (2008)	2.822	3	0.025
Campbell and Bozorgnia (2008)	2.977	2	0.017
Zhao et al. (2006)	3.078	1	0.008
Normal Fault			
Model	LLH	Rank	Weight
Campbell and Bozorgnia (2003); Present Study	2.037	13	0.143
Atkinson and Boore (2006); Present Study	2.206	12	0.132
Anbazhagan et al. (2013)	2.218	11	0.121
Raghukanth and Kavitha (2014)	2.243	10	0.110
NDMA (2010)	2.315	9	0.099
Toro (2002)	2.322	8	0.088
Akkar and Bommer (2010)	2.357	7	0.077
Lin and Lee (2008)	2.412	6	0.066
Chiou and Youngs (2008)	2.433	5	0.055
Zhao et al. (2006)	2.539	4	0.044
Atkinson and Boore (2006)	2.547	3	0.033
Abrahamson and Silva (2008)	2.595	2	0.022
Campbell and Bozorgnia (2008)	2.652	1	0.011

Table S7. The weights and ranks assigned to respective GMPEs based on the average LLH ranking in the four seismogenic zones for Northeast India Tectonic Province

Eastern Himalayan Seismogenic Zone (EHZ)

Model	LLH	Rank	Weight
Campbell and Bozorgnia (2003); Present Study	2.168	5	0.33
Atkinson and Boore (2006); Present Study	2.236	4	0.27
Anbazhagan et al. (2013)	2.268	3	0.20
Nath et al. (2012)	2.438	2	0.13
Toro (2002)	2.656	1	0.07
Mishmi Block Seismogenic Zone (MBZ)			
Model	LLH	Rank	Weight
Campbell and Bozorgnia (2003); Present Study	2.243	5	0.33
Atkinson and Boore (2006); Present Study	2.333	4	0.27
Nath et al. (2012)	2.570	3	0.20
Youngs et al. (1997)	2.573	2	0.13
Gupta (2010)	2.760	1	0.07
Eastern Boundary Seismogenic Zone (EBZ)			
Model	LLH	Rank	Weight
Campbell and Bozorgnia (2003); Present Study	2.369	5	0.33
Atkinson and Boore (2006); Present Study	2.370	4	0.27
Singh et al. (2016)	2.635	3	0.20
Gupta (2010)	2.712	2	0.13
Youngs et al. (1997)	2.786	1	0.07
Shillong Seismogenic Zone (SHZ)			
Model	LLH	Rank	Weight
Campbell and Bozorgnia (2003); Present Study	2.316	5	0.33
Atkinson and Boore (2006); Present Study	2.323	4	0.27
Nath et al. (2012)	2.425	3	0.20
Youngs et al. (1997)	2.705	2	0.13
Singh et al. (2016)	2.748	1	0.07

Table S8. Pairwise comparison matrix and normalized weights assigned to the GMPEs used for Northwest India seismogenic source zone

Model	Campbell and Bozorgnia (2003)	Atkinson and Boore (2006)	Harbindu et al. (2014)	Anbazhagan et al. (2013)	Raghukanth and Kavitha (2014)	Weight
Campbell and Bozorgnia (2003)	1	5/4	5/3	5/2	5/1	0.33
Atkinson and Boore (2006)	4/5	1	4/3	4/2	4/1	0.27

Harbindu et al. (2014)	3/5	3/4	1	3/2	3/1	0.20
Anbazhagan et al. (2013)	2/5	2/4	2/3	1	2/1	0.13
Raghukanth and Kavitha (2014)	1/5	1/4	1/3	1/2	1	0.07

Reviewer#2: The section of damage analysis is quite incomplete since there is no specific discussion on the type of buildings present in the area and on their seismic and structural characteristics.

Authors' Response: The following text has been incorporated in the electronic supplement of the revised manuscript:

Structural Impact Assessment in terms of Damage Potential Modelling and Human Casualty Assessment in cities of the seismogenic Tectonic Ensemble from Kashmir Himalaya to Northeast India:

(i) Building identification and classification following FEMA (2000) and WHE-PAGER (2008) nomenclature using Google Earth Imagery with due validation performed using Rapid Visual Screening, (RVS) on 25% samples of the entire ensemble and establishing user and producer accuracy and Kappa Statistics as enunciated below.

The seismic resistant capability of a building is closely related to its structural type. The damage of a building depends on a number of factors including building type, building height, building age, building floor area, etc. In the present study, the building typology is classified based on the following image processing-cum accuracy assessment protocol given in **Figure S7.**

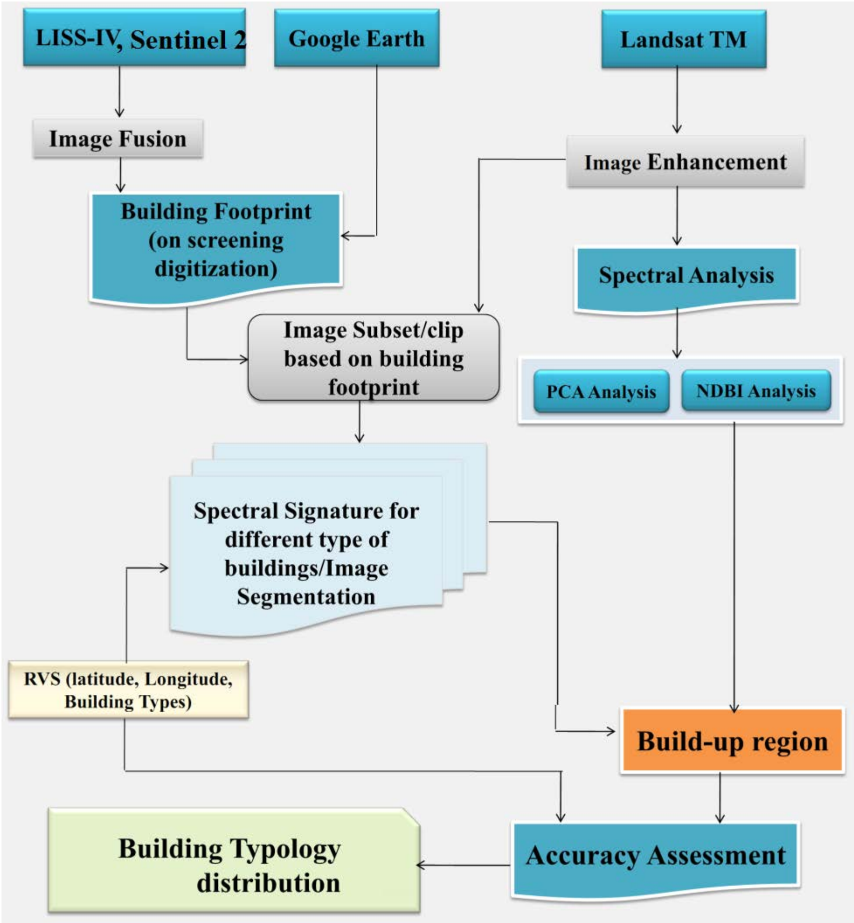

Figure S7. Building typology classification based on hybrid Remote Sensing and RVS processing.

These are further sub-classified using building height through the following protocol that uses Google Earth 2011 and Cartosat I Stereo Image shown in **Figure S8** to yield FEMA (2000) & WHE-PAGER (2008) nomenclature based building typology and those used in the present study for seismic structural impact assessment.

\

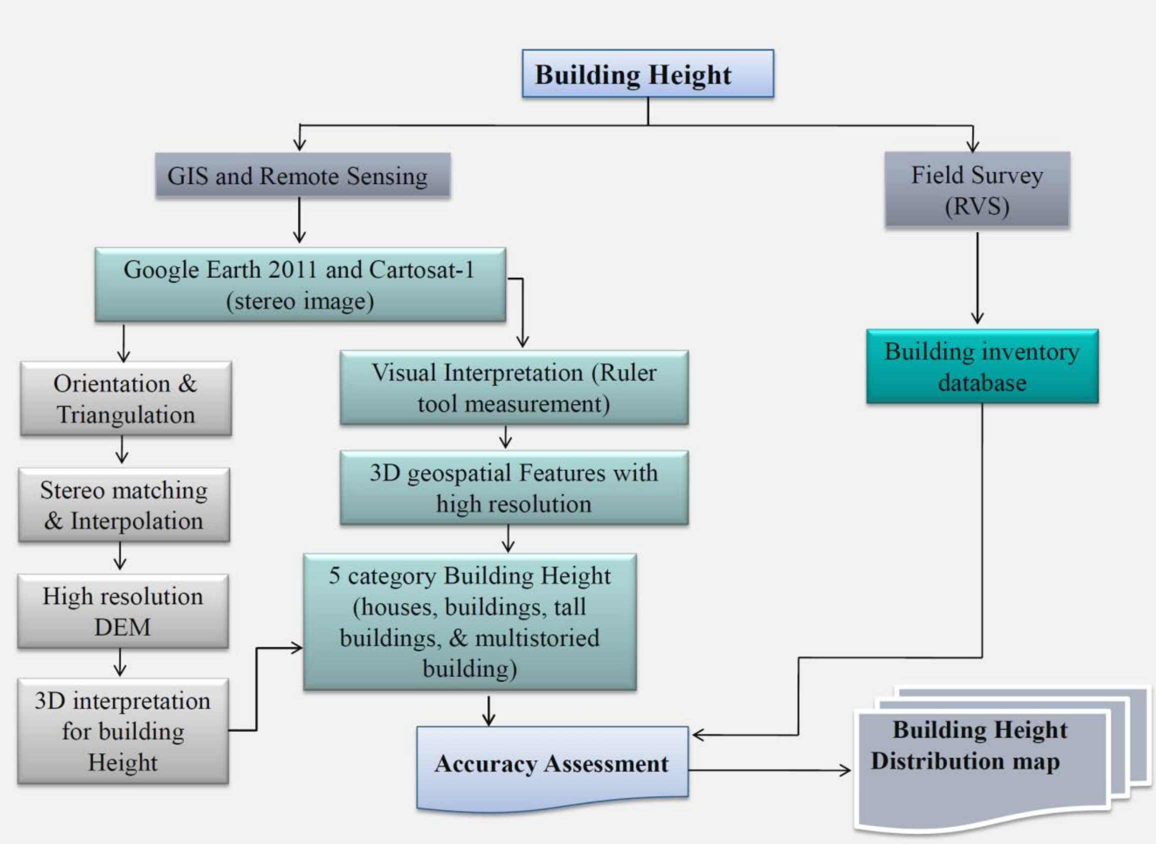

Figure S8. Building sub-classification protocol based on Building Height.

The most common way of representing the confidence level in the assessment of remote sensing data is in the form of computing an error matrix. It is based on the widely used accuracy assessment technique of statistical correlations between two data sets –one is the Rapid Visual Screening (RVS) of about 25-30% samples in the study region as shown in **Figure S9**, which we term as 'reference' and the other derived exclusively from remotely sensed data, which is termed as 'classified'. The correlation indicators used in the present analysis include "overall accuracy", i.e., the percentage of matched data between the 'reference' and the 'classified' data, "user's accuracy", i.e., the percentage of matched data in the 'classified' map, "producer's accuracy", i.e., the percentage of matched data in the 'reference' map.

In the present study, the structural vulnerability exposures derived from satellite imagery in case of building typology classified from Google Earth 3-D aspect, Sentinel 2, LISS IV and Cartosat I for building height etc. are used as 'classified' data while those derived through Rapid Visual Screening from 25000 field survey locations in the ensemble being considered as 'reference' data have been used for the accuracy assessment of all the themes as given in **Tables S13** and **S14**.

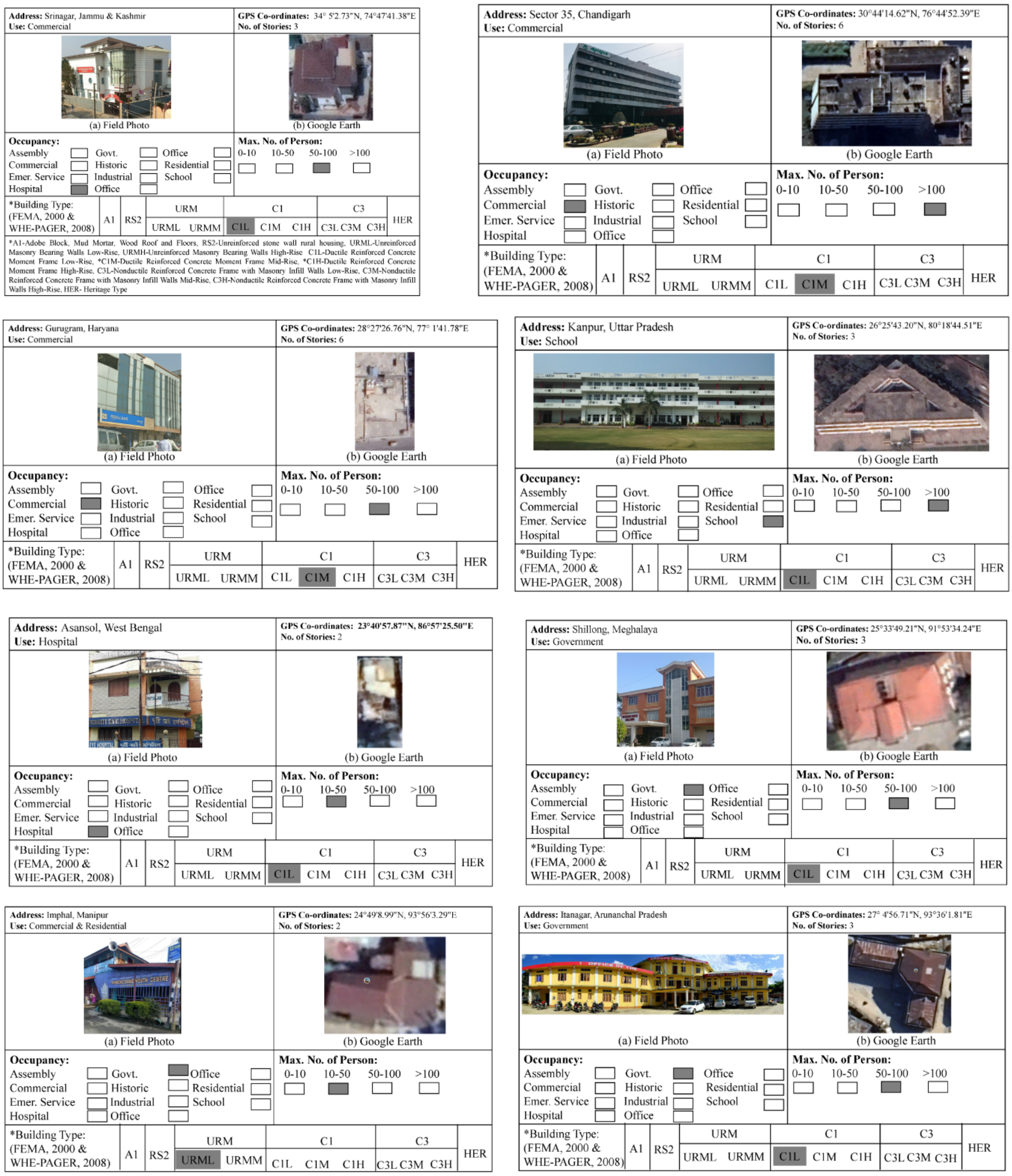

Figure S9. Rapid Visual Screening (RVS) survey for field and satellite imagery comparisons of existing building type and height in selected urban centers.

Table S13. Error matrix derived for building height.

Classified Building Height	RVS based Building Height (Reference data)							User's Accuracy (%)
		Houses	Buildings	Tall Buildings	Multistoried Buildings	Skyscrapers	Total	
	Houses (1 Floor)	205	47	0	0	0	252	81.34

	Buildings (2-4 Floors)	25	149	15	0	0	189	78.84
	Tall Buildings (5-8 Floors)	0	5	105	23	0	133	78.94
	Multistoried Buildings (9-10 Floors)	0	0	15	63	0	78	80.76
	Skyscrapers (>10 Floors)	0	0	0	0	10	10	100
	Total	230	201	135	86	10		
Producer's Accuracy (%)		89.13	74.13	77.78	73.26	100		
Overall Accuracy (%)								80.36

Table S14. Error matrix derived for building typology

		RVS based building typology (Reference data)												User's Accuracy (%)
		A1	RS2	URMM	URML	C1L	C1M	C1H	C3L	C3M	C3H	HER	Total	
Classified building typology	A1	15	4	1	0	0	0	0	0	0	0	0	20	75.00
	RS2	10	70	6	0	0	0	0	0	0	0	0	86	81.40
	URMM	5	17	100	20	0	0	0	0	0	0	0	142	70.42
	URML	0	3	43	189	8	0	0	0	0	0	0	243	77.78
	C1L	0	0	8	21	156	4	0	0	0	0	0	189	82.54
	C1M	0	0	0	2	31	120	9	0	0	0	0	162	74.07
	C1H	0	0	0	0	4	15	90	0	0	0	0	109	82.57
	C3L	0	0	0	0	0	0	10	107	2	0	0	119	89.92
	C3M	0	0	0	0	0	0	0	7	19	87	0	113	76.99
	C3H	0	0	0	0	0	0	0	0	7	63	0	70	90.00
	HER	0	0	0	0	0	0	0	0	0	0	5	5	100.00
	Total	30	94	158	232	199	139	109	114	96	82	5		

Producer's Accuracy (%)	50.00	74.47	63.29	81.47	78.39	86.33	82.57	93.86	90.63	76.83	100.00		
Overall Accuracy (%):													79.65

Finally, thus through RVS, Google Earth 3-D aspect, Sentinel 2, LISS IV and Cartosat I Imagery analyses we detected 11 model building types in the entire tectonic ensemble as tabulated in **Table S15.**

Table S15. Different model building types used in the present study (FEMA, 2000; WHE-PAGER, 2008).

Model Building Type	Description	Height	Stories
HER	Heritage building		
C1L	Ductile reinforced concrete frame with or without infill	Low-Rise	1 – 3
C1M		Mid-Rise	4 - 6
C1H		High-Rise	7+
C3L	Non-ductile reinforced concrete frame with masonry infill walls	Low-Rise	1 - 3
C3M		Mid-Rise	4 - 6
C3H		High-Rise	7+
A1	Adobe Block, Mud Mortar, Wood Roof and Floors	Low-Rise	1-2
RS2	Rubble stone masonry walls with timber frame and roof	Low-Rise	1-2
URML	Unreinforced masonry bearing wall	Low-Rise	1-3
URMM		Mid-Rise	3+

(i) Generation of Damage Probability in the three tectonic territories viz. West-Northwest India, North-Central Himalaya and Northeast India including Nepal, Bhutan and Bangladesh

Damageability functions, defined as the probability of sustaining any damage are obtained by plotting damage probability against intensity or any other ground shaking parameters like PGA, PGV, PGD as had been worked out by Gautam et al. (2021) for stone masonry buildings in Nepal considering 1934 Bihar-Nepal earthquake of M_w 8.1, 1988 Nepal-Bihar earthquake of M_w 6.9 and 2015 Gorkha-Nepal earthquake of M_w 7.8 wherein 95-100% of this building type defined by FEMA (2000), WHE-PAGER (2008) as URM type had been projected to have been damaged for a GMPE predicted PGA value of 0.78g. Following suggestions from the Reviewer and taking clue from the works of Gautam et al. (2021) a rigorous literature survey has been conducted by us as detailed below and damage data have been collected as reported to have been inflicted by large and great Historical earthquakes in Nepal, Bhutan as suggested by the Reviewer and also extended the effort to the three seismogenic tectonic territories of the present ensemble viz. West-Northwest Himalaya, North-Central Himalaya and Northeast India and worked out damageability functions in all of them for three model building typologies viz. Adobe (A1), Unreinforced Masonry (URM) bearing structures and Reinforced Concrete (RC) structures in the ensemble.

As we are all aware, the entire Himalayan belt frequently experiences major earthquakes due to continuous convergence of Indian plate beneath the Eurasian plate. Nepal, being centrally located in the belt, is worst affected. The number of buildings damaged during 1833 Nepal earthquake of M_w 7.6 is about 18,000 in the Kathmandu valley. The 1934 Bihar-Nepal earthquake of M_w 8.1 affected 200,000 buildings in the eastern mountains of Nepal and northern Bihar of India. 1966 Bajhang earthquake of M_w 6.3 damaged 7844 buildings in the western Nepal as reported by Bilham (1995), Pandey & Molnar (1988) and Chaulagain et al. (2018) for these earthquakes respectively. A1 and URM-type buildings were mostly prevalent in those regions at the time when the aforementioned earthquakes jolted those territories. 1980 Chainpur earthquake of M_w 6.5 is the only major event that occurred in the western section of the central seismic gap and Singh (1982) reported that approximately 32,186 buildings were damaged during that earthquake. The 1988 Nepal-Bihar earthquake of M_w 6.9 damaged about 70,000 buildings and triggered widespread liquefaction in eastern Nepal as documented by Gupta (1988) and Fujiwara et al. (1989). The recent earthquake damage statistics are available at the Nepal Disaster Risk Reduction Portal (http://drrportal.gov.np/). The 2011 Sikkim earthquake of M_w 6.9 and 2015 Gorkha-Nepal earthquake of M_w 7.8 have also been considered in the present study for structural impact assessment.

This work has been extended for the North-Central Himalaya region and it is found that Bihar and Uttar Pradesh of India have been remarkably affected by the same earthquakes. Dasgupta and Mukhopadhay (2015) has assembled all the reports and commentaries on 1833 Nepal earthquake of M_w 7.6 and it is reported that in the towns of Munger, Muzaffarpur, Arrah and Gorakhpur there had been building damages. There had been reporting of 149124 buildings in Bihar being damaged during 1988 Nepal-Bihar Earthquake of M_w 6.9. About 145 adobe-type buildings were damaged in Northern Bihar due to 2015 Gorkha-Nepal Earthquake of M_w 7.8.

The Northeast India region including Bhutan have repeatedly been struck by devastating earthquakes causing significant damage to life and properties. The District Disaster Management Department of the Government of Bhutan reported district-wise building damage due to past devastating earthquakes occurring in the region like, approximately 251 A1 and RC-type buildings getting damaged due to 2003 Paro earthquake of M_w 5.5, around 126 URM and RC-type buildings getting damaged due to 2006 Dewangthang earthquake of M_w 5.8 and about 5967 buildings getting damaged due to 2009 Bhutan earthquake of M_w 6.1. Chettri et al. (2021) presented an overview of seismic vulnerability of Bhutanese residential buildings and reported that 4950 buildings were damaged during 2009 Bhutan earthquake of M_w 6.1 and 7965 buildings were damaged during 2011 Sikkim earthquake of M_w 6.9. According to Gautam et al. (2022), 60% of all buildings in Bhutan were exposed to 2021 Sonitpur earthquake of M_w 6.4, among those 16 buildings collapsed, 541 buildings sustained major damage and 2277 buildings sustained minor damage. Halder et al. (2020) reported the extent of damage caused to buildings of various typologies by large earthquakes that occurred in Northeast India, amongst which 6727 mud-walled (Adobe-type) houses suffered partial to complete damage in the state of Tripura consequent upon 2017 Ambasa earthquake of M_w 5.7 while slight to moderate damage occurred to the houses due to the impact of 2016 Manipur earthquake of M_w 6.7 in Imphal, 2021 Sonitpur earthquake of M_w 6.4 in and around Sonitpur in Assam and 2011 Sikkim earthquake of M_w 6.9 in Sikkim. Damages have been reported by Debbarma et al. (2021) and Dey et al. (2022). The National Disaster Management Authority has reported maximum damage in North Sikkim region where 78%, 70% and 60% of A1, URM and RC type buildings have been damaged respectively due to 2011 Sikkim earthquake of M_w 6.9 while the West and East Sikkim also experienced considerable damage. According to Dutta et al. (2015), 2422 buildings have been damaged in Gangtok itself.

West-Northwest Himalaya has been jolted by numerous earthquakes from historic times. Mukhopadhyay and Dasgupta (2015) has compiled the extent of damage caused due to impact of large historical earthquakes in and around Kashmir and Kangra Valley viz. 1803 Garhwal earthquake of M_w 7.5, 1828 Srinagar earthquake of M_w 6.5 and 1905 Kangra earthquake of M_w 7.8. The Kinnaur and Lahul-Spiti districts of Himachal Pradesh were severely affected by 1975 Kinnaur earthquake of M_w 6.8 heavily damaging about 2000 houses in that around the region as reported by Singh et al. (1976) and Bhargava et al. (1978). The 1991 Uttarkashi earthquake of M_w 6.8 has rocked Garhwal Himalaya of Northern India with MM intensity of VIII causing complete collapse of 20184 houses and partially damaging 74714 houses (Arya, 1994). District-wise number of building damages has been documented in a report published by Geological Survey of India (GSI, 1992). Pandey (2013) reported that damage was observed in more than 64000 unreinforced masonry buildings as well as reinforced concrete frame structures. Himachal Pradesh State Disaster Management Authority (https://hpsdma.nic.in/) has reported that more than 70% houses developed cracks in the epicentral region during 1995 Chamba earthquake of M_w 4.9, maximum damage being experienced in Pilure-Baraur sector located 8-10 km northeast of Chamba town as reported by Mahajan (1998). Field observations after 1997 Sundernagar earthquake of M_w 4.7 in Sundernagar region and around Mandi district of Himachal Pradesh have been compiled by Thakur et al. (1997) reporting extensive damages to about 1000 adobe houses and developing small cracks in concrete structures. A report by Paul (2000) on 1999 Chamoli earthquake of M_w 6.5 has detailed the damages observed in the Chamoli region. Several such accounts have been collected regarding 2004 Dharamshala earthquake of M_w 4.9, 2005 Muzaffarabad earthquake of M_w 7.6, 2012 Jhajjar earthquake of M_w 5.1, 2013 Bhaderwah-Kishtwar earthquake of M_w 5.1 and 2019 Kashmir earthquake of M_w 5.6 with reporting of considerable damage to unreinforced masonry and reinforced concrete buildings prevalent in recent times. The 2005 Muzaffarabad earthquake of M_w 7.6, the worst ever earthquake that shook the Kashmir valley with its epicentre located 124 km to the west of Srinagar, caused widespread destruction and casualties (>50,000) in the region as detailed in Mahajan (2006). Kumar and Murty (2014) reported that about 450000 houses have been destroyed in Kashmir. Gupta et al. (2013) has compiled all the reports in context of 2012 Jhajjar earthquake of M_w 5.1 affecting the Haryana-Delhi border region depicting the damage patterns along with MM intensity variation of III-VI in the region due to this earthquake.

Based on the reported number of buildings damaged during impinging large, strong and great earthquakes against the total number of buildings actually existent in the same period extracted through remote sensing technique using the imagery data prevalent during that particular period Damage Probability has been calculated and plotted against the Modified Mercalli Intensity (MMI) for North-Central Himalaya, Nepal, Northeast India, Bhutan and West-Northwest India as presented in **Figures 22(a-c)**, **23(a-c)**, **24(a-c)**, **25(a-c)** and **26(a-c)** respectively for Adobe(A1), Unreinforced Masonry (URM) and Reinforced Concrete (RC) model building types for these tectonic territories in the ensemble. We invoked SELENA (Molina et al., 2014) package for assessing damage states for A1, URM and RC type buildings for all the scenario earthquakes as well as the surface-consistent probabilistic seismic hazard in terms of surface level PGA(g) distribution in all these territories and ascertained the damage state domains for these three building types A1, URM and RC in all the territories and juxtaposed the same tectonic territory-wise on each of these diagrams as shown in **Figures 22, 23, 24, 25** and **26** depicting the four damage states viz. ‘Slight’, ‘Moderate’, ‘Extensive’ and ‘Complete’ for all the three model building types. It is evident from these diagrams that all building damages reported by till date for all the aforementioned earthquakes have been classified in the SELENA modelled four damage state domains in all the aforementioned tectonic territories, thus, bringing in a good agreement between the SELENA generated building damage state for A1, URM and RC-type buildings and damage probability distribution variation against Modified Mercalli Intensity and/or equivalent converted PGA(g) in all the three seismogenic tectonic territories including Nepal and Bhutan for all the scenario earthquakes as well as surface-consistent probabilistic seismic hazard distribution.

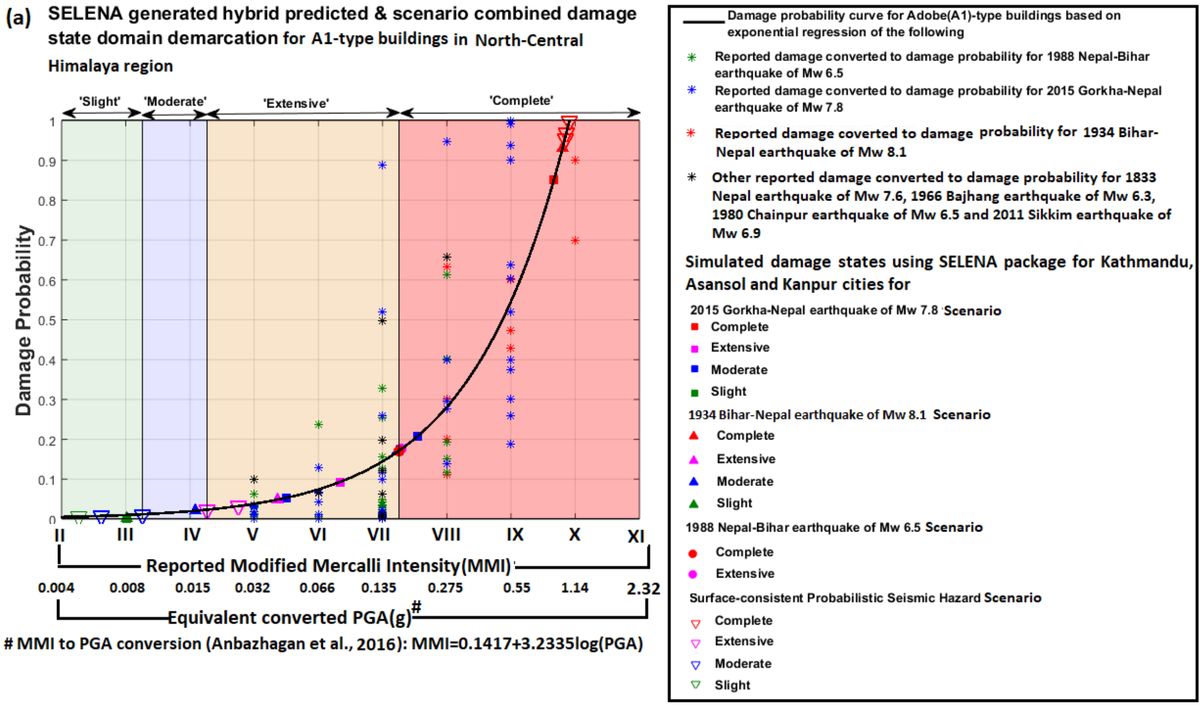
(a)
SELENA generated hybrid predicted & scenario combined damage state domain demarcation for A1-type buildings in North-Central Himalaya region
'Slight'
'Moderate'
'Extensive'
'Complete'
Damage Probability
0
0.1
0.2
0.3
0.4
0.5
0.6
0.7
0.8
0.9
1
II
III
IV
V
VI
VII
VIII
IX
X
XI
Reported Modified Mercalli Intensity(MMI)
0.004
0.008
0.015
0.032
0.066
0.135
0.275
0.55
1.14
2.32
Equivalent converted PGA(g)#
MMI to PGA conversion (Anbazhagan et al., 2016): MMI=0.1417+3.2335log(PGA)
Damage probability curve for Adobe(A1)-type buildings based on exponential regression of the following
Reported damage converted to damage probability for 1988 Nepal-Bihar earthquake of Mw 6.5
Reported damage converted to damage probability for 2015 Gorkha-Nepal earthquake of Mw 7.8
Reported damage coverted to damage probability for 1934 Bihar-Nepal earthquake of Mw 8.1
Other reported damage converted to damage probability for 1833 Nepal earthquake of Mw 7.6, 1966 Bajhang earthquake of Mw 6.3, 1980 Chainpur earthquake of Mw 6.5 and 2011 Sikkim earthquake of Mw 6.9
Simulated damage states using SELENA package for Kathmandu, Asansol and Kanpur cities for
2015 Gorkha-Nepal earthquake of Mw 7.8 Scenario
Complete
Extensive
Moderate
Slight
1934 Bihar-Nepal earthquake of Mw 8.1 Scenario
Complete
Extensive
Moderate
Slight
1988 Nepal-Bihar earthquake of Mw 6.5 Scenario
Complete
Extensive
Surface-consistent Probabilistic Seismic Hazard Scenario
Complete
Extensive
Moderate
Slight

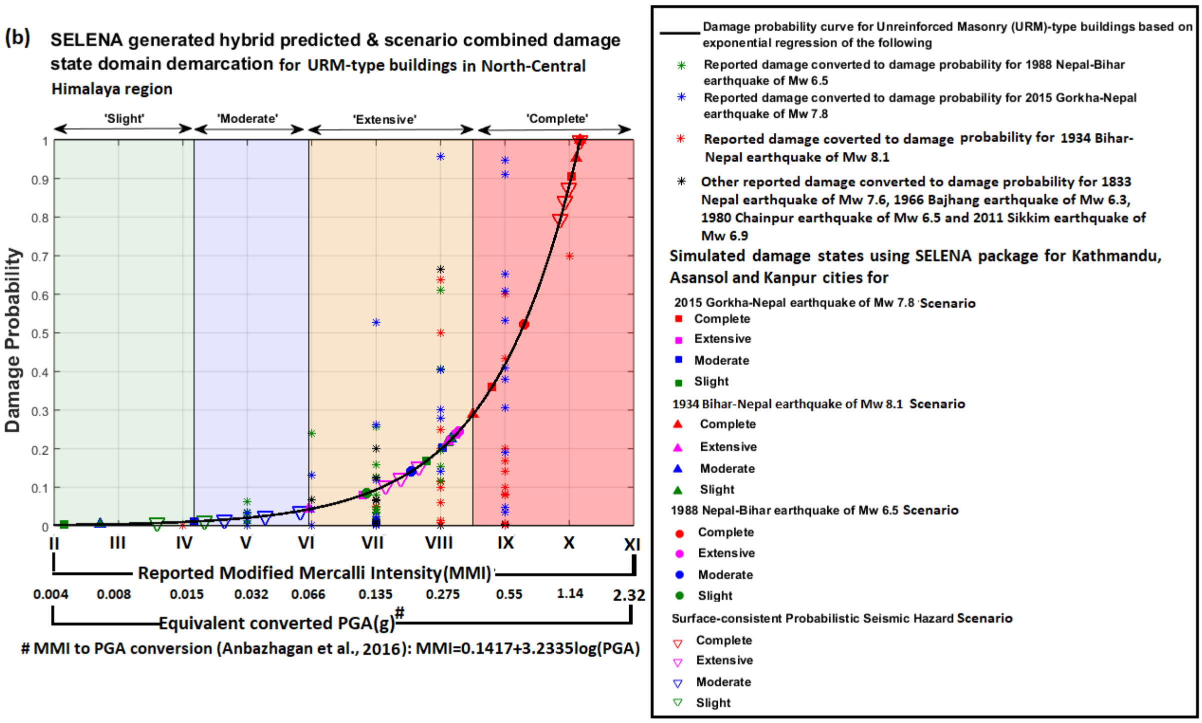
(b)
SELENA generated hybrid predicted & scenario combined damage state domain demarcation for URM-type buildings in North-Central Himalaya region
'Slight'
'Moderate'
'Extensive'
'Complete'
Damage Probability
0
0.1
0.2
0.3
0.4
0.5
0.6
0.7
0.8
0.9
1
II
III
IV
V
VI
VII
VIII
IX
X
XI
Reported Modified Mercalli Intensity(MMI)
0.004
0.008
0.015
0.032
0.066
0.135
0.275
0.55
1.14
2.32
Equivalent converted PGA(g)#
MMI to PGA conversion (Anbazhagan et al., 2016): MMI=0.1417+3.2335log(PGA)
Damage probability curve for Unreinforced Masonry (URM)-type buildings based on exponential regression of the following
Reported damage converted to damage probability for 1988 Nepal-Bihar earthquake of Mw 6.5
Reported damage converted to damage probability for 2015 Gorkha-Nepal earthquake of Mw 7.8
Reported damage coverted to damage probability for 1934 Bihar-Nepal earthquake of Mw 8.1
Other reported damage converted to damage probability for 1833 Nepal earthquake of Mw 7.6, 1966 Bajhang earthquake of Mw 6.3, 1980 Chainpur earthquake of Mw 6.5 and 2011 Sikkim earthquake of Mw 6.9
Simulated damage states using SELENA package for Kathmandu, Asansol and Kanpur cities for
2015 Gorkha-Nepal earthquake of Mw 7.8 Scenario
Complete
Extensive
Moderate
Slight
1934 Bihar-Nepal earthquake of Mw 8.1 Scenario
Complete
Extensive
Moderate
Slight
1988 Nepal-Bihar earthquake of Mw 6.5 Scenario
Complete
Extensive
Moderate
Slight
Surface-consistent Probabilistic Seismic Hazard Scenario
Complete
Extensive
Moderate
Slight

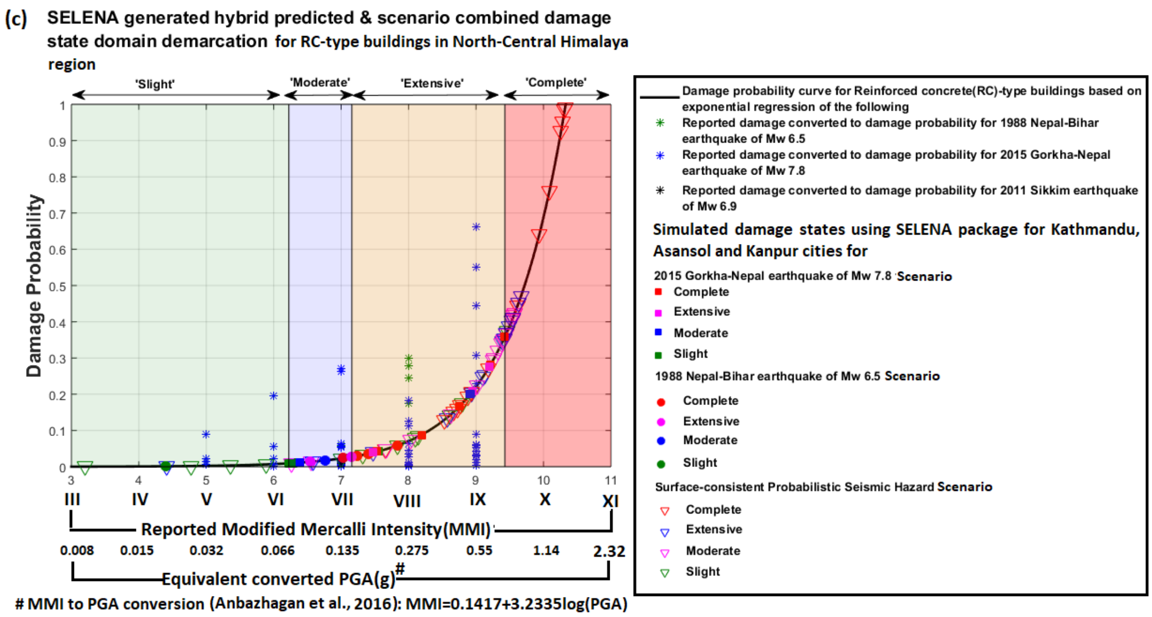

Figure 22. Damage probability curve for North-Central Himalaya region for (a) Adobe (A1), (b) Unreinforced Masonry (URM) and (c) Reinforced Concrete (RC)-type buildings based on exponential regression of reported damage converted to damage probability for different earthquake scenarios. SELENA generated hybrid predicted and scenario combined damage states have been demarcated based on simulated damage states for three earthquake scenarios viz. 1934 Bihar-Nepal earthquake of M_w 8.1, 1988 Nepal-Bihar earthquake of M_w 6.9 and 2015 Gorkha-Nepal earthquake of M_w 7.8 and Surface-consistent Probabilistic Seismic Hazard scenario.

(a) SELENA generated hybrid predicted & scenario combined damage state domain demarcation for A1-type buildings in Nepal region

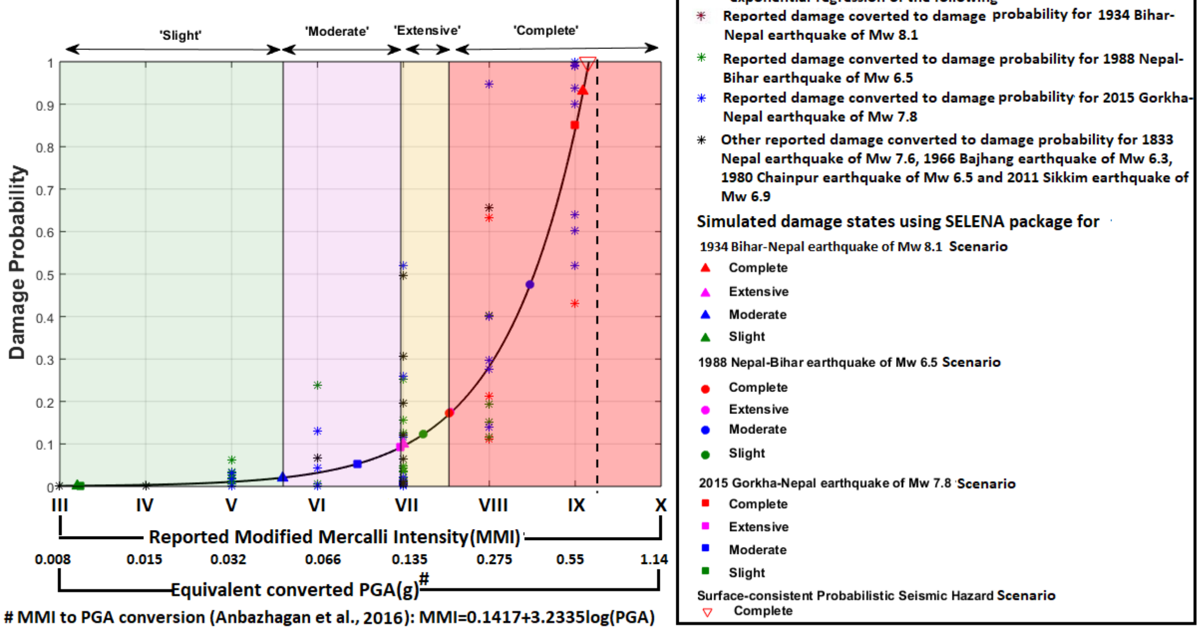

MMI to PGA conversion (Anbazhagan et al., 2016): MMI=0.1417+3.2335log(PGA)

(b) SELENA generated hybrid predicted & scenario combined damage state domain demarcation for URM-type buildings in Nepal

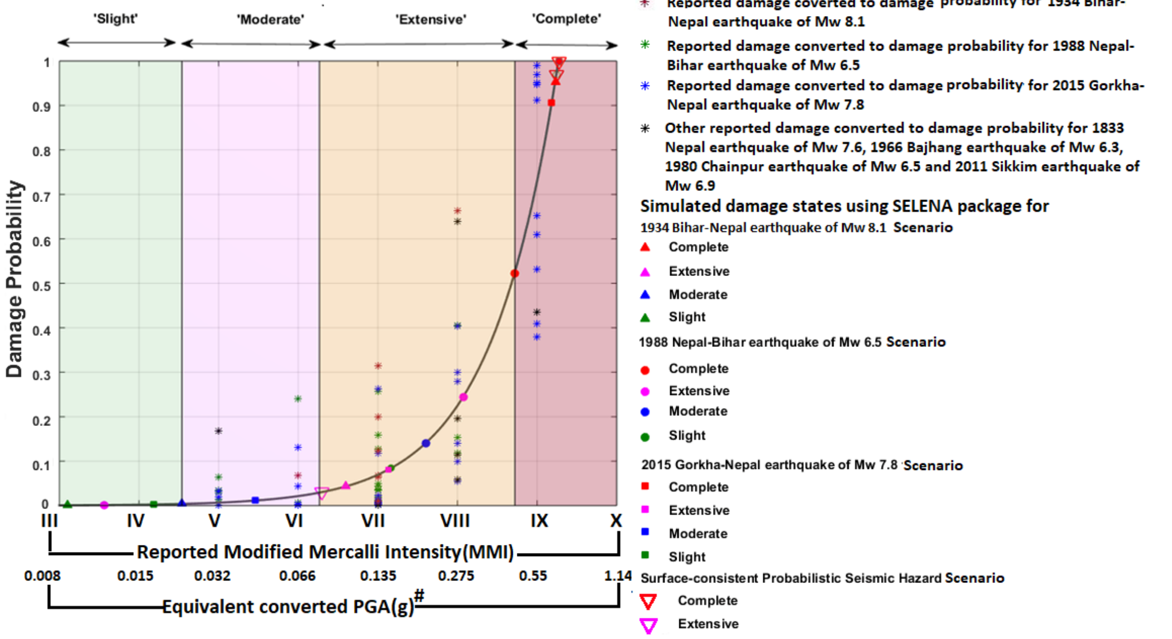

MMI to PGA conversion (Anbazhagan et al., 2016): MMI=0.1417+3.2335log(PGA)

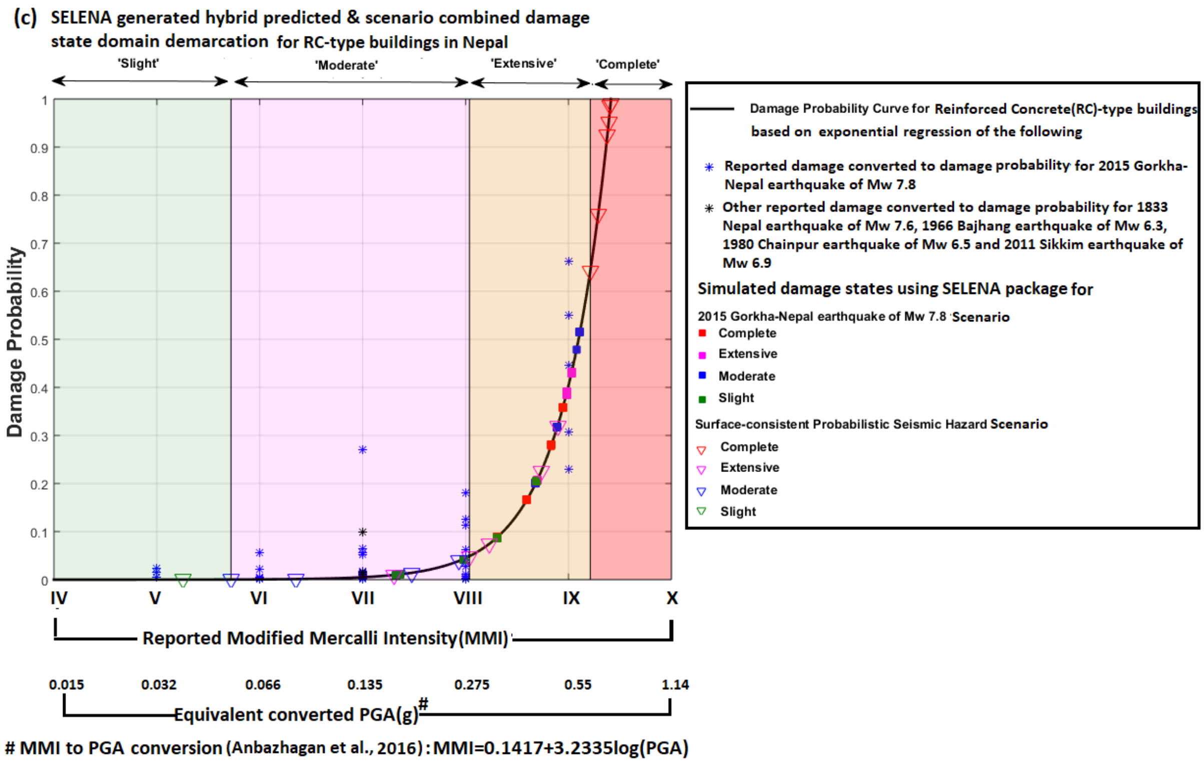

Figure 23. Damage probability curves for Nepal region for (a) Adobe (A1), (b) Unreinforced Masonry (URM) and (c) Reinforced Concrete (RC)-type buildings based on exponential regression of reported damage converted to damage probability for different earthquake scenarios. SELENA generated hybrid predicted and scenario combined damage states have been demarcated based on simulated damage states for three earthquake scenarios viz. 1934 Bihar-Nepal earthquake of M_w 8.1, 1988 Nepal-Bihar earthquake of M_w 6.9 and 2015 Gorkha-Nepal earthquake of M_w 7.8 and Surface-consistent Probabilistic Seismic Hazard scenario.

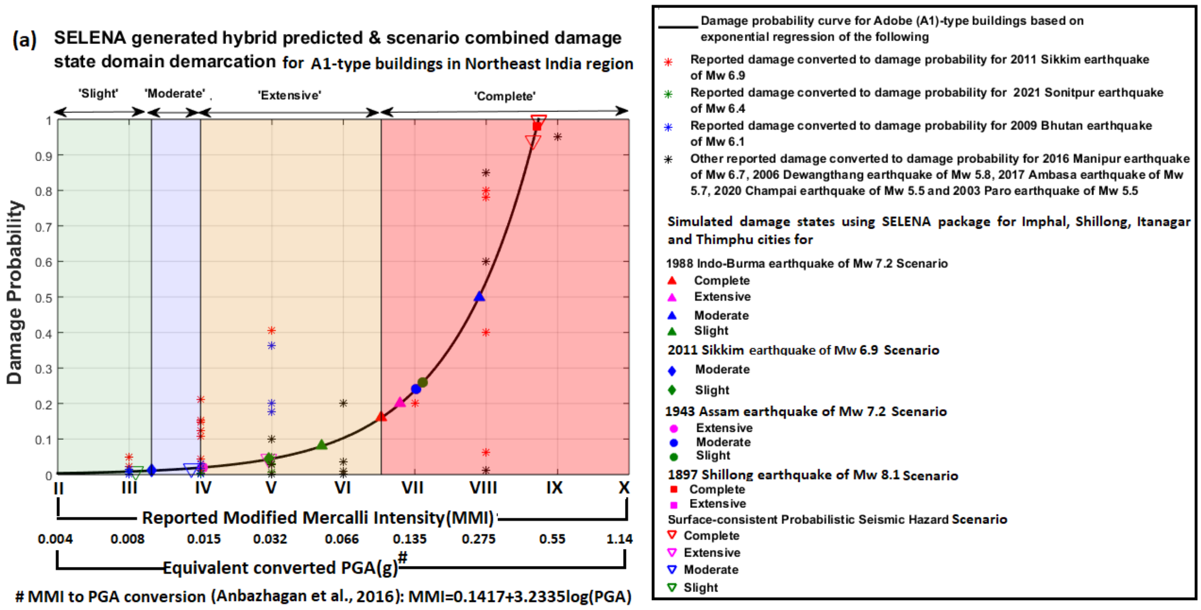
(a) SELENA generated hybrid predicted & scenario combined damage state domain demarcation for A1-type buildings in Northeast India region
'Slight'
'Moderate'
'Extensive'
'Complete'
Damage Probability
1
0.9
0.8
0.7
0.6
0.5
0.4
0.3
0.2
0.1
0
II
III
IV
V
VI
VII
VIII
IX
X
Reported Modified Mercalli Intensity(MMI)
0.004
0.008
0.015
0.032
0.066
0.135
0.275
0.55
1.14
Equivalent converted PGA(g)#
MMI to PGA conversion (Anbazhagan et al., 2016): MMI=0.1417+3.2335log(PGA)
Damage probability curve for Adobe (A1)-type buildings based on exponential regression of the following
Reported damage converted to damage probability for 2011 Sikkim earthquake of Mw 6.9
Reported damage converted to damage probability for 2021 Sonitpur earthquake of Mw 6.4
Reported damage converted to damage probability for 2009 Bhutan earthquake of Mw 6.1
Other reported damage converted to damage probability for 2016 Manipur earthquake of Mw 6.7, 2006 Dewangthang earthquake of Mw 5.8, 2017 Ambasa earthquake of Mw 5.7, 2020 Champai earthquake of Mw 5.5 and 2003 Paro earthquake of Mw 5.5
Simulated damage states using SELENA package for Imphal, Shillong, Itanagar and Thimphu cities for
1988 Indo-Burma earthquake of Mw 7.2 Scenario
Complete
Extensive
Moderate
Slight
2011 Sikkim earthquake of Mw 6.9 Scenario
Moderate
Slight
1943 Assam earthquake of Mw 7.2 Scenario
Extensive
Moderate
Slight
1897 Shillong earthquake of Mw 8.1 Scenario
Complete
Extensive
Surface-consistent Probabilistic Seismic Hazard Scenario
Complete
Extensive
Moderate
Slight

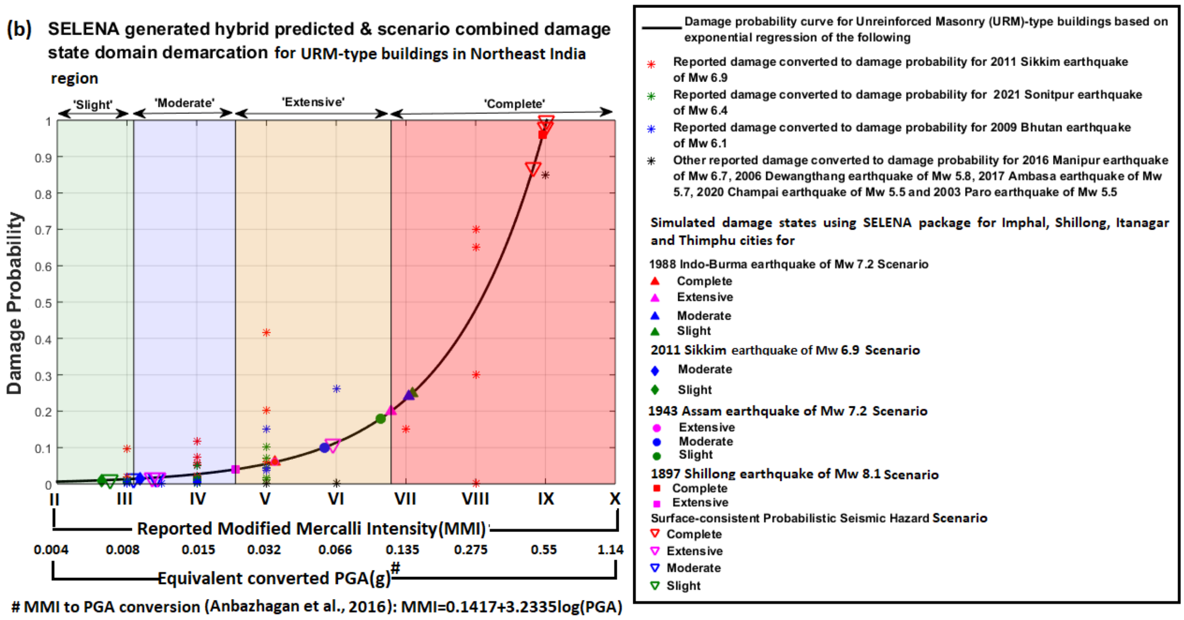
(b) SELENA generated hybrid predicted & scenario combined damage state domain demarcation for URM-type buildings in Northeast India region
'Slight'
'Moderate'
'Extensive'
'Complete'
Damage Probability
1
0.9
0.8
0.7
0.6
0.5
0.4
0.3
0.2
0.1
0
II
III
IV
V
VI
VII
VIII
IX
X
Reported Modified Mercalli Intensity(MMI)
0.004
0.008
0.015
0.032
0.066
0.135
0.275
0.55
1.14
Equivalent converted PGA(g)#
MMI to PGA conversion (Anbazhagan et al., 2016): MMI=0.1417+3.2335log(PGA)
Damage probability curve for Unreinforced Masonry (URM)-type buildings based on exponential regression of the following
Reported damage converted to damage probability for 2011 Sikkim earthquake of Mw 6.9
Reported damage converted to damage probability for 2021 Sonitpur earthquake of Mw 6.4
Reported damage converted to damage probability for 2009 Bhutan earthquake of Mw 6.1
Other reported damage converted to damage probability for 2016 Manipur earthquake of Mw 6.7, 2006 Dewangthang earthquake of Mw 5.8, 2017 Ambasa earthquake of Mw 5.7, 2020 Champai earthquake of Mw 5.5 and 2003 Paro earthquake of Mw 5.5
Simulated damage states using SELENA package for Imphal, Shillong, Itanagar and Thimphu cities for
1988 Indo-Burma earthquake of Mw 7.2 Scenario
Complete
Extensive
Moderate
Slight
2011 Sikkim earthquake of Mw 6.9 Scenario
Moderate
Slight
1943 Assam earthquake of Mw 7.2 Scenario
Extensive
Moderate
Slight
1897 Shillong earthquake of Mw 8.1 Scenario
Complete
Extensive
Surface-consistent Probabilistic Seismic Hazard Scenario
Complete
Extensive
Moderate
Slight

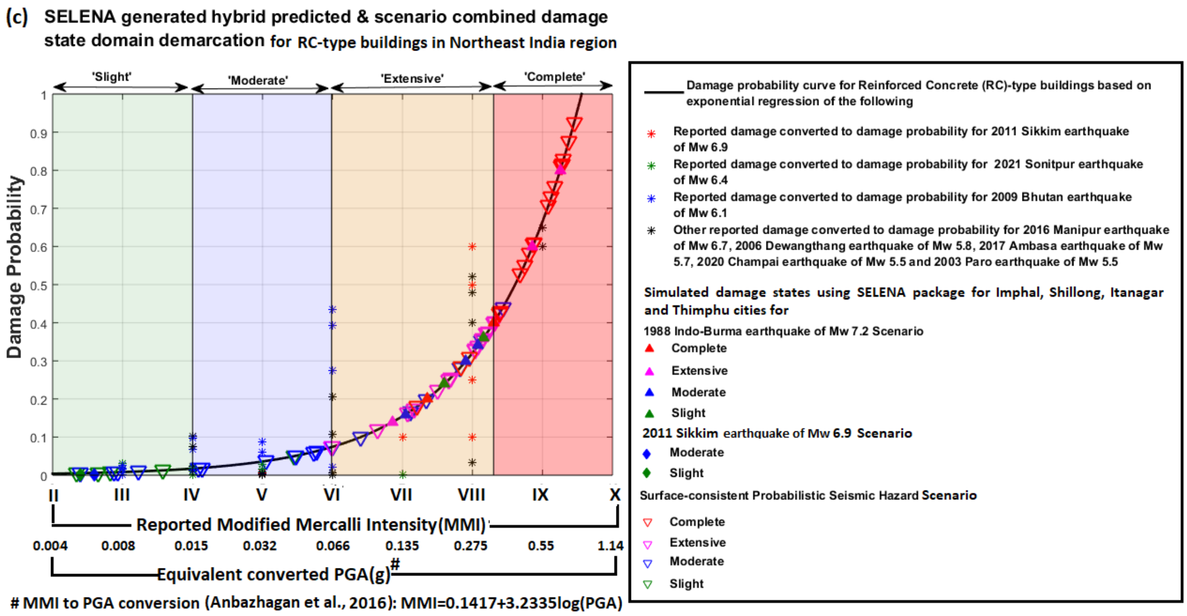

Figure 24. Damage probability curve for Northeast India region for (a) Adobe (A1), (b) Unreinforced Masonry (URM) and (c) Reinforced Concrete (RC)-type buildings based on exponential regression of reported damage converted to damage probability for different earthquake scenarios. SELENA generated hybrid predicted and scenario combined damage states have been demarcated based on simulated damage states for Four earthquake scenarios viz. 1897 Shillong earthquake of M_w 8.1, 1943 Assam earthquake of M_w 7.2, 1988 Indo-Burma earthquake of M_w 7.2 and 2011 Sikkim earthquake of M_w 6.9 and Surface-consistent Probabilistic Seismic Hazard scenario.

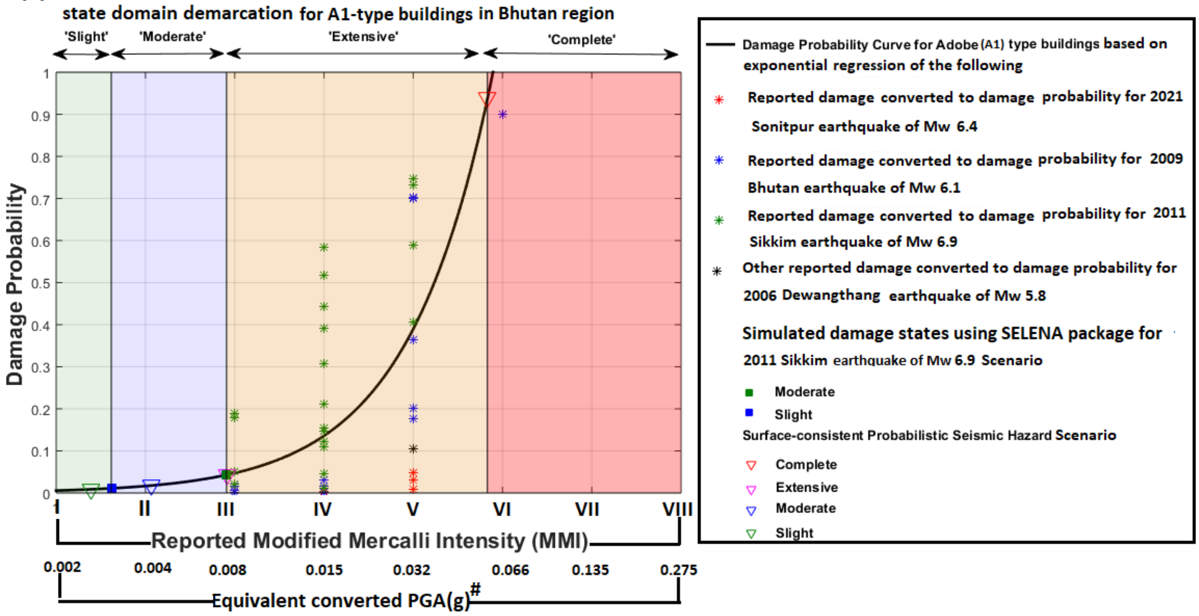

(a) SELENA generated hybrid predicted & scenario combined damage state domain demarcation for A1-type buildings in Bhutan region

MMI to PGA conversion(Anbazhagan et al., 2016): MMI=0.1417+3.2335log(PGA)

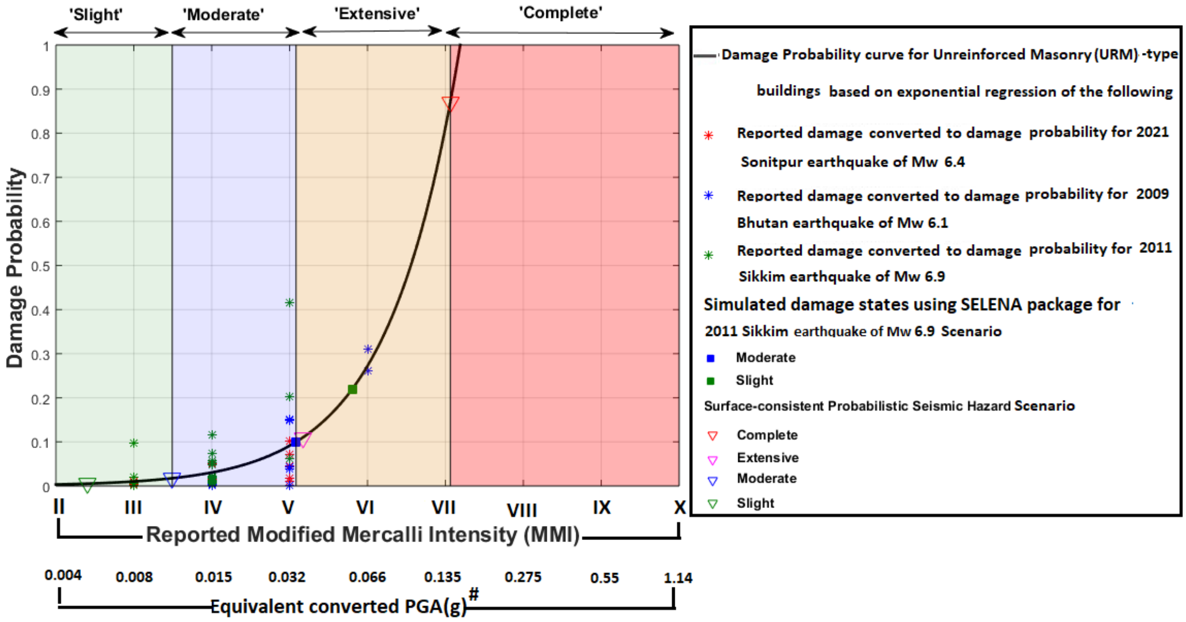

(b) SELENA generated hybrid predicted & scenario combined damage state domain demarcation for URM-type buildings in Bhutan region

MMI to PGA conversion(Anbazhagan et al., 2016): MMI=0.1417+3.2335log(PGA)

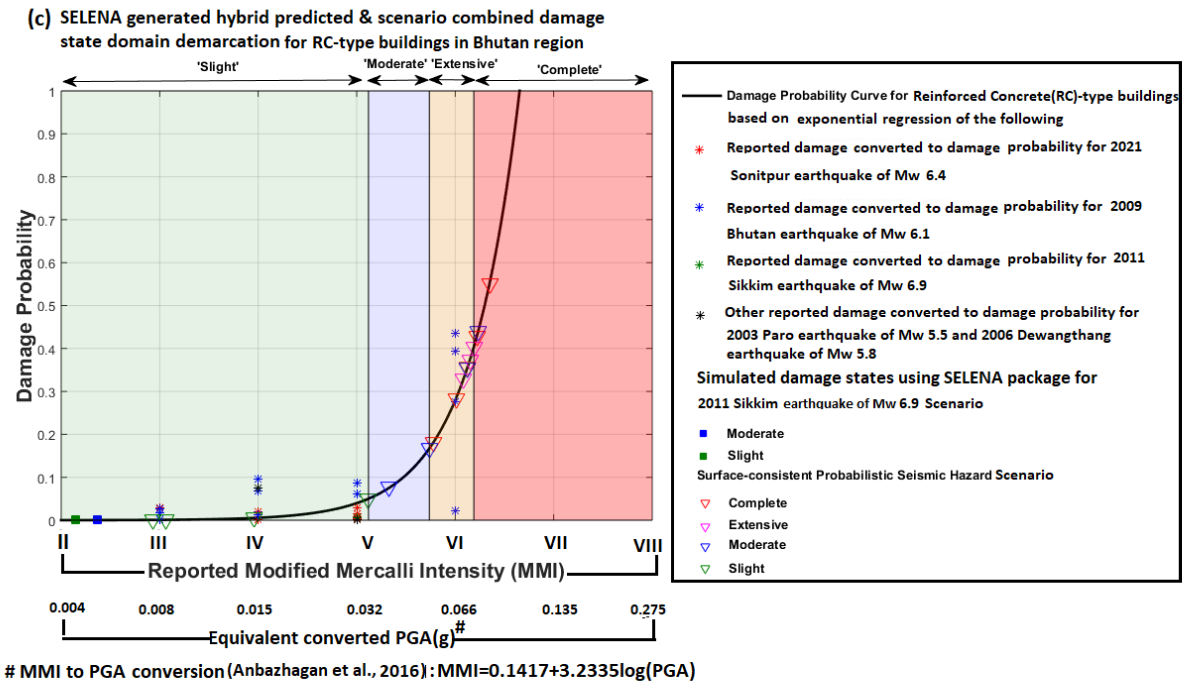

Figure 25. Damage probability curve for Bhutan region for (a) Adobe (A1), (b) Unreinforced Masonry (URM) and (c) Reinforced Concrete (RC)-type buildings based on exponential regression of reported damage converted to damage probability for different earthquake scenarios. SELENA generated hybrid predicted and scenario combined damage states have been demarcated based on simulated damage states for the 2011 Sikkim earthquake of M_w 6.9 and Surface-consistent Probabilistic Seismic Hazard scenario.

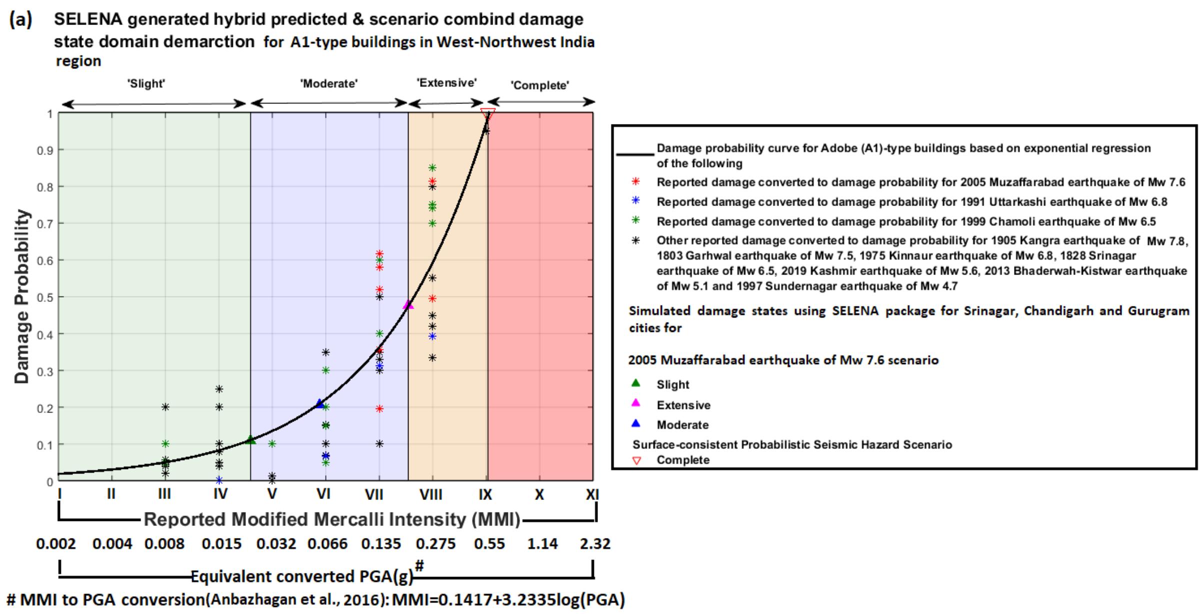

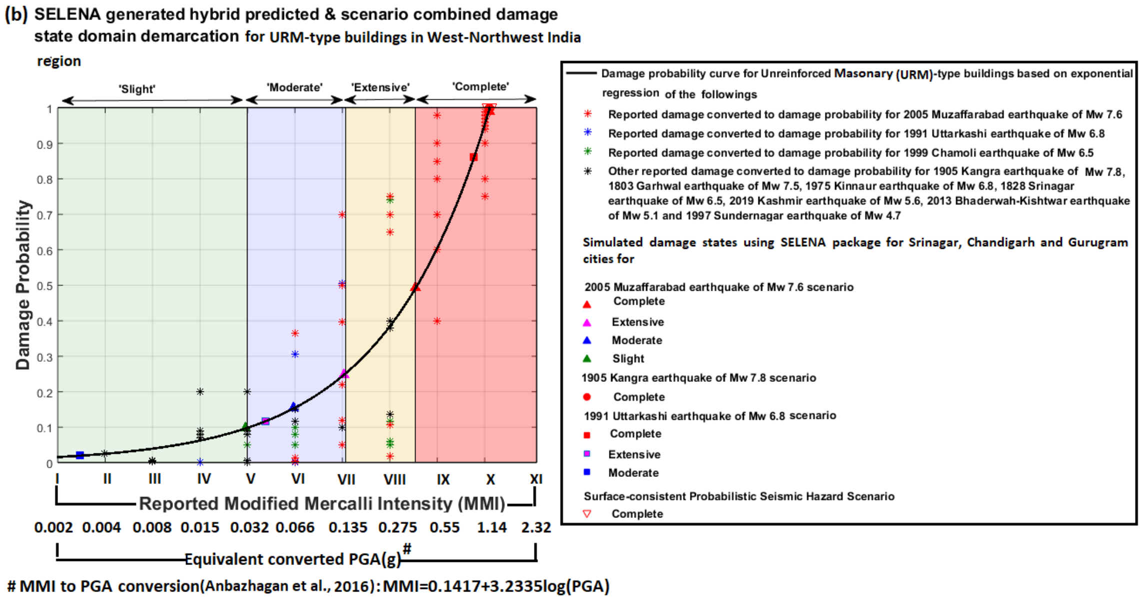

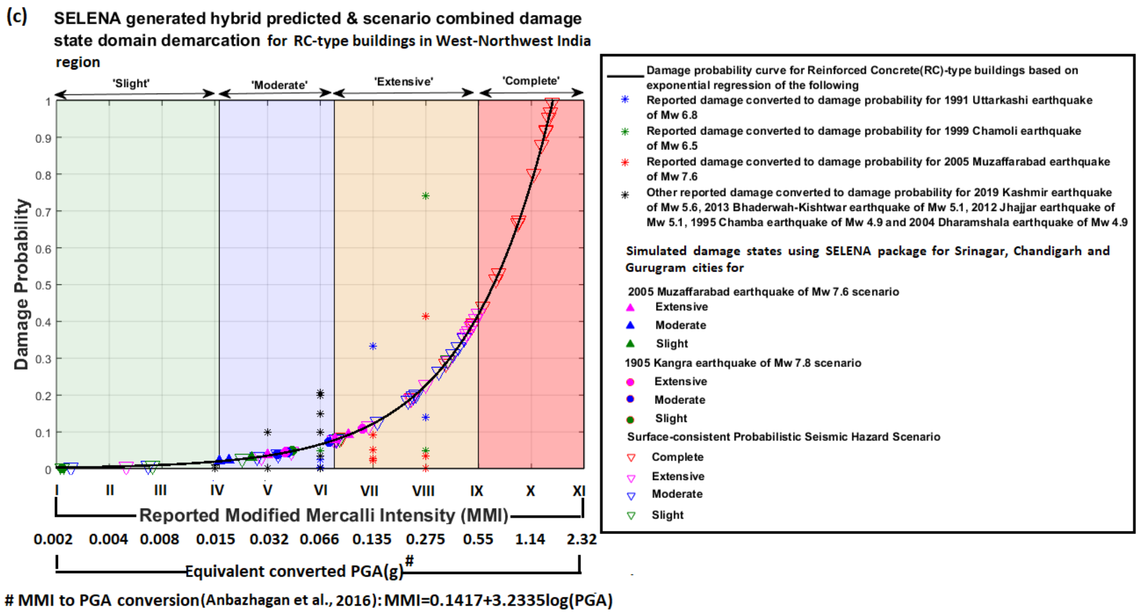

Figure 26. Damage probability curve for West-Northwest India region for (a) Adobe (A1), (b) Unreinforced Masonry (URM) and (c) Reinforced Concrete (RC)-type buildings based on exponential regression of reported damage converted to damage probability for different earthquake scenarios. SELENA generated hybrid predicted and scenario combined damage states have been demarcated based on simulated damage states for three earthquake scenarios viz. 1905 Kangra earthquake of M_w 7.8, 1991 Uttarkashi earthquake of M_w 6.8 and 2005 Muzaffarabad earthquake of M_w 7.6 and Surface-consistent Probabilistic Seismic Hazard scenario.

References:

Abrahamson, N. and Silva, W.: Summary of the Abrahamson & Silva NGA ground-motion relations, Earthquake Spectra, 24(1), 67-97, https://doi.org/10.1193%2F1.2924360, 2008.

Adhikari, M. D. and Nath, S. K.: Site-specific next generation ground motion prediction models for Darjeeling-Sikkim Himalaya using strong motion seismometry, Journal of Indian Geophysical Union, 20(2), 151-170, 2016.

Akkar, D. S. and Bommer, J. J.: Empirical equations for the prediction of PGA, PGV, and spectral accelerations in Europe, the Mediterranean region, and the Middle East, Seismological Research Letters, 81 (2), 195–206, https://doi.org/10.1785/gssrl.81.2.195, 2010.

Anbazhagan, P., Kumar, A., and Sitharam, T. G.: Ground motion prediction equation considering combined dataset of recorded and simulated ground motions, Soil Dynamics and Earthquake Engineering, 53, 92-108, https://doi.org/10.1016/j.soildyn.2013.06.003, 2013.

Arya, A. S.: October 20, 1991 Uttarkashi (India) earthquake, Earthquake Engineering, 10th World Conference©1994 Balkema, Rotterdam, pp. 7039-7043, 1994.

Atkinson, G. M. and Boore, D. M.: Earthquake ground-motion prediction equations for eastern North America, Bulletin of the seismological society of America, 96(6), 2181-2205, https://doi.org/10.1785/0120050245, 2006.

Bhargava, O. N., Ameta, S. S., Gaur, R. K., Kumar, S., Agrawal, A. N., Jalote, P. M., and Sadhu, M. L.: The Kinnaur (HP India) earthquake of 19 January 1975: summary of geoseismological observations, Bulletin of the Indian Geological Association, 11(1), 39-53, 1978.

Bilham, R.: Location and magnitude of the 1833 Nepal earthquake and its relation to the rupture zones of contiguous great Himalayan earthquakes, Current Science, 69(2), 101-128, 1995.

Boore, D. M. and Atkinson, G. M.: Ground-motion prediction equations for the average horizontal component of PGA, PGV, and 5%-damped PSA at spectral periods between 0.01 s and 10.0s, Earthquake spectra, 24(1), 99-138, https://doi.org/10.1193%2F1.2830434, 2008.

BSSC: NEHRP recommended provisions for seismic regulations for new buildings and other structures. 2003 Edition, Part 1: Provisions, Building Seismic Safety Council for the Federal Emergency Management Agency (Report FEMA 450), and Washington D.C., https://www.nehrp.gov/, 2003.

Campbell, K. W. and Bozorgnia, Y.: NGA ground motion model for the geometric mean horizontal component of PGA, PGV, PGD and 5% damped linear elastic response spectra for periods ranging from 0.01 to 10s, Earthquake spectra, 24(1), 139-171, https://doi.org/10.1193%2F1.2857546, 2008.

Campbell, K. W. and Bozorgnia, Y.: Updated near-source ground-motion (attenuation) relations for the horizontal and vertical components of peak ground acceleration and acceleration response spectra, Bulletin of the Seismological Society of America, 93(1), 314-331, https://doi.org/10.1785/0120020029, 2003.

Census: Census of India 2011. Provisional Population Totals, New Delhi: Government of India, 409-413, 2011.

Chaulagain, H., Gautam, D., and Rodrigues, H.: Revisiting major historical earthquakes in Nepal: Overview of 1833, 1934, 1980, 1988, 2011, and 2015 seismic events, Impacts and insights of the Gorkha earthquake, 1-17, https://doi.org/10.1016/B978-0-12-812808-4.00001-8, 2018.

Chettri, N., Gautam, D., and Rupakhety, R: Seismic Vulnerability of Vernacular Residential Buildings in Bhutan, Journal of Earthquake Engineering, 1-16, https://doi.org/10.1080/13632469.2020.1868362, 2021.

Chiou, B. J. and Youngs, R. R.: An NGA model for the average horizontal component of peak ground motion and response spectra, Earthquake spectra, 24(1), 173-215, https://doi.org/10.1193%2F1.2894832, 2008.

Dasgupta, S., and Mukhopadhyay, B.: Historiography and commentary from archives on the Kathmandu (Nepal)–India earthquake of 26 August 1833, Indian Journal of History of Science (INSA), 50, 491-513, https://doi.org/10.13140/RG.2.1.4088.2726 , 2015.

Debbarma, J., and Debnath, J.: Assessment on the impact of the Tripura earthquake (January 3, 2017, M_w= 5.6) in Northeast India, Journal of the Geographical Institute "Jovan Cvijić" SASA, 71(1), 1-13, https://doi.org/10.2298/IJGI2101001D, 2021.

Dey, Chandan, Santanu Baruah, Mohamed F. Abdelwahed, Sowrav Saikia, Nabajyoti Molia, Prachurjya Borthakur, Timangshu Chetia et al.: The 28 April 2021 Kopili Fault Earthquake (M_w 6.1) in Assam Valley of North East India: Seismotectonic Appraisal. Pure and Applied Geophysics, 1-16, 2022.

FEMA: Prestandard and commentary for the Seismic Rehabilitation of Buildings, Federal Emergency Management Agency 356, Washington D.C., 2000.

Frankel, A.: Mapping seismic hazard in the central and eastern United States. Seismological Research Letters, 66(4), 8-21, 1995.

Fujiwara, T., Sato, T., Murakami, H.O., Kubo. T.: Reconnaissance Report on the 21 August 1988 Earthquake in the Nepal-India Border Region, Research Report on Natural Disasters. Japanese Group for the Study of Natural Disaster Science, Tokyo, Japan, 1989.

Gautam, D, Rupakhety, R., Adhikari, R., Shrestha, B. C., Baruwal, R. and Bhatt, L.: "Seismic vulnerability of Himalayan stone masonry: Regional perspectives." In Masonry Construction in Active Seismic Regions, pp. 25-60. Woodhead Publishing, 2021.

Gautam, D., Chettri, N., Tempa, K., Rodrigues, H., and Rupakhety, R.: Seismic vulnerability of bhutanese vernacular stone masonry buildings: From damage observation to fragility analysis, Soil Dynamics and Earthquake Engineering, 160, 107351, https://doi.org/10.1016/j.soildyn.2022.107351, 2022.

Grünthal, G.: European macroseismic scale 1998, European Seismological Commission (ESC), 1998.

GSI: A report on intensity surveys carried out for Uttarkashi earthquake of October 20, 1991, Geological Survey of India, special publication no. 30, 1992.

Gupta, A. K., Chopra, S., Prajapati, S. K., Sutar, A. K., and Bansal, B. K. (2013), Intensity distribution of M 4.9 Haryana–Delhi border earthquake, Natural hazards, 68(2), 405-417.

Gupta, I. D.: Response spectral attenuation relations for in-slab earthquakes in Indo-Burmese subduction zone, Soil Dynamics and Earthquake Engineering, 30(5), 368-377, https://doi.org/10.1016/j.soildyn.2009.12.009, 2010.

Gupta, S. P.: Report on Eastern Nepal Earthquake of 21 August 1~ 88, Damages and Recommendations for Repairs and Reconstruction, Asian Disaster Preparedness Center, Asian Institute of Technology, Bangkok, Thailand, 1988.

Halder, L., Dutta, S. C., and Sharma, R. P.: Damage study and seismic vulnerability assessment of existing masonry buildings in Northeast India, Journal of Building Engineering, 29, 101190, 2020.

Harbindu, A., Gupta, S., and Sharma, M. L.: Earthquake ground motion predictive equations for Garhwal Himalaya, India, Soil Dynamics and Earthquake Engineering, 66, 135-148, https://doi.org/10.1016/j.soildyn.2014.06.018, 2014.

Hasancebi, N., and Ulusay, R.: Empirical correlations between shear wave velocity and penetration resistance for ground shaking assessments, Bulletin of Engineering Geology and the Environment, 66(2), 203-213, https://doi.org/10.1007/s10064-006-0063-0, 2007.

Hwang, H. and Huo, J. R.: Attenuation relations of ground motion for rock and soil sites in eastern United States, Soil Dynamics and Earthquake Engineering, 16(6), 363-372, https://doi.org/10.1016/S0267-7261(97)00016-X, 1997.

Kumar, R. P., and Murty, C. V. R.: Earthquake safety of houses in India: understanding the bottlenecks in implementation, Indian Concrete Journal, 1, 2014.

Lin, P. S. and Lee, C. T.: Ground-motion attenuation relationships for subduction-zone earthquakes in northeastern Taiwan, Bulletin of the Seismological Society of America, 98(1), 220-240, https://doi.org/10.1785/0120060002, 2008.

Mahajan, A. K.: The 24th March, 1995 Chamba earthquake (NW Himalaya), field observations and seismotectonics, Journal of the Geological Society of India, 51(2), 227-232, 1998.

Mahajan, A. K., Kumar, N., and Arora, B. R.: Quick look isoseismal map of 8 October 2005 Kashmir earthquake, Current Science, 356-361, 2006.

Maiti, S. K., Nath, S. K., Adhikari, M. D., Srivastava, N., Sengupta, P., and Gupta, A. K.: Probabilistic seismic hazard model of West Bengal, India, Journal of Earthquake Engineering, 21(7), 1113-1157, https://doi.org/10.1080/13632469.2016.1210054, 2017.

Martin, S., and Szeliga, W.: A catalog of felt intensity data for 570 earthquakes in India from 1636 to 2009, Bulletin of the Seismological Society of America, 100(2), 562-569, https://doi.org/10.1785/0120080328, 2010.

Molina, S., Lang, D. H., and Lindholm, C. D.: SELENA v6.0: User and Technical Manual v6.0, Report no. 14-003, Kjeller (Norway) – Alicante (Spain), 102, 2014.

Mukhopadhyay, B., and Dasgupta, S.: Seismic hazard assessment of Kashmir and Kangra valley region, Western Himalaya, India, Geomatics, Natural Hazards and Risk, 6(2), 149-183, https://doi.org/10.1080/19475705.2013.832405, 2015.

Nath, S. K., Adhikari, M. D., Devaraj, N., and Maiti, S. K.: Seismic vulnerability and risk assessment of Kolkata City, India, Natural Hazards Earth System Sciences, 15, 1103–1121, https://doi.org/10.5194/nhess-15-1103-2015, 2015.

Nath, S. K., Adhikari, M. D., Maiti, S. K., and Ghatak, C.: Earthquake hazard potential of Indo-Gangetic Foredeep: its seismotectonism, hazard, and damage modeling for the cities of Patna, Lucknow, and Varanasi, Journal of Seismology, 23(4), 725-769, https://doi.org/10.1007/s10950-019-09832-3, 2019.

Nath, S. K., Adhikari, M. D., Maiti, S. K., Devaraj, N., Srivastava, N., and Mohapatra, L. D.: Earthquake scenario in West Bengal with emphasis on seismic hazard microzonation of the city of Kolkata, India, Natural Hazards and Earth System Sciences, 14, 2549–2575, https://doi.org/10.5194/nhess-14-2549-2014, 2014.

Nath, S. K., and Thingbaijam, K. K. S.: Peak ground motion predictions in India: an appraisal for rock sites, Journal of Seismology, 15(2), 295-315, https://doi.org/10.1007/s10950-010-9224-5, 2011.

Nath, S. K., Raj, A., Thingbaijam, K. K. S., and Kumar, A.: Ground Motion Synthesis and Seismic Scenario in Guwahati City—A Stochastic Approach, Seismological Research Letters, 80 (2): 233–242, https://doi.org/10.1785/gssrl.80.2.233, 2009.

Nath, S. K., Thingbaijam, K. K. S., Maiti, S. K., and Nayak, A.: Ground-motion predictions in Shillong region, northeast India, Journal of seismology, 16(3), 475-488, https://doi.org/10.1007/s10950-012-9285-8, 2012.

Nath, S. K., Mandal, S., Adhikari, M. D., and Maiti, S. K.: A Unified Earthquake Catalogue for South Asia covering the period 1900-2014, Natural Hazards, 85(3), 1787-1810, https://doi.org/10.1007/s11069-016-2665-6, 2017.

Nath, S. K.: Probabilistic Seismic Hazard Atlas of 40 Cities in India, © Ministry of Earth Sciences, Government of India, New Delhi, 457p, 2017.

Nath, S. K., Ghatak, C., Sengupta, A., Biswas, A., Madan, J., and Srivastava, A.: Regional–Local Hybrid Seismic Hazard and Disaster Modeling of the Five Tectonic Province Ensemble Consisting of Westcentral Himalaya to Northeast India. In: Sitharam T., Jakka R., Kolathayar S. (eds) Latest Developments in Geotechnical Earthquake Engineering and Soil Dynamics, Springer Transactions in Civil and Environmental Engineering. Springer, Singapore, 14, 307-358. https://doi.org/10.1007/978-981-16-1468-2_14, 2021.

NDMA.: Development of probabilistic seismic hazard map of India, Technical Report Published by Govt. of India, New Delhi, Working committee of experts (WCE), NDMA, 2010.

Pandey, M. R., and Molnar, P.: The distribution of intensity of the Bihar-Nepal earthquake of 15 January 1934 and bounds on the extent of the rupture zone, Journal of Nepal Geological Society, 5(1), 22-44, 1988.

Pandey, R. J.: Natural Disasters and Risk Assessment in Uttarakhand with special reference to Uttarkashi Earthquake, IOSR Journal of Humanities and Social Science (IOSR-JHSS), 9(3), 37-42, 2013.

Paul, D. K.: A report on Chamoli earthquake of March 29, 1999, Department of Earthquake Engineering, University of Roorkee, 2000.

Raghukanth, S. T. G. and Iyengar, R. N.: Estimation of seismic spectral acceleration in peninsular India, Journal of Earth System Science, 116(3), 199-214, https://doi.org/10.1007/s12040-007-0020-8, 2007.

Raghukanth, S. T. G. and Kavitha, B.: Ground motion relations for active regions in India, Pure and Applied Geophysics, 171(9), 2241-2275, https://doi.org/10.1007/s00024-014-0807-x, 2014.

Saaty, T. L.: The Analytic Hierarchy Process, McGraw-Hill International, New York, U.S.A, 1980.

Sadigh, K., Chang, C. Y., Egan, J. A., Makdisi, F., and Youngs, R. R.: Attenuation relationships for shallow crustal earthquakes based on California strong motion data, Seismological research letters, 68(1), 180-189, https://doi.org/10.1785/gssrl.68.1.180, 1997.

Scherbaum, F., Delavaud, E., and Riggelsen, C.: Model selection in seismic hazard analysis: An information-theoretic perspective, Bulletin of the Seismological Society of America, 99(6), 3234-3247, https://doi.org/10.1785/0120080347, 2009.

Sharma, M. L., Douglas, J., Bungum, H., and Kotadia, J.: Ground-Motion Prediction Equations Based on Data from the Himalayan and Zagros Regions, Journal of Earthquake Engineering, 13(8), 1191-1210, https://doi.org/10.1080/13632460902859151, 2009.

Sharma, M. L., Harbindu, A., and Kamal: Strong ground motion prediction equation for Northwest Himalayan region based on stochastic approach, In: Proceedings of 15th World Conference of Earthquake Engineering, Lisbon, 2012.

Singh, N. M., Rahman, T., and Wong, I. G.: A New Ground Motion Prediction Model for Northeastern India (NEI) Crustal Earthquakes, Bulletin of the Seismological Society of America, 106(3), 1282-1297, https://doi.org/10.1785/0120150180, 2016.

Singh, S., Jain, A. K., Sinha, P., Singh, V. N., and Srivastava, L. S. The Kinnaur earthquake of January 19, 1975: A field report, Bulletin of the Seismological Society of America, 66(3), 887-901, 1976.

Singh, V.: Earthquake of July 1980 in far western Nepal, Journal of Nepal Geological Society, 2(2), 1-11. https://doi.org/10.3126/jngs.v2i2.32530, 1982.

Sun, C. G., Kim, H. S., Cho, H. I.: Geo-Proxy-Based Site Classification for Regional Zonation of Seismic Site Effects in South Korea, Applied Sciences, 8(2), 314, https://doi.org/10.3390/app8020314, 2018.

Thakur, V. C., Mahajan, A. K., Mundepi, A. K., SriRam, V., Pandey, H.C., and Singh, R.: The Sundernagar earthquake (NW Himalaya) of 29th July, 1997 field observations and seismotectonics, Wadia Institute of Himalayan Geology, Dehradun, 1997.

Toro, G. R.: Modification of the Toro et al. (1997) attenuation equations for large magnitudes and short distances, Risk Engineering Technical Report, 10, 2002.

WHE-PAGER: WHE-PAGER Phase 2, Development of Analytical Seismic Vulnerability Functions, EERI-WHE-US Geological Survey, 2008.

Youngs, R. R., Chiou, S. J., Silva, W. J., and Humphrey, J. R.: Strong ground motion attenuation relationships for subduction zone earthquakes, Seismological research letters, 68(1), 58-73, https://doi.org/10.1785/gssrl.68.1.58, 1997.

Zhao, J. X., Zhang, J., Asano, A., Ohno, Y., Oouchi, T., Takahashi, T., Ogawa, H., Irikura, K., Thio, H. K., Somerville, P. G., Fukushima, Y., and Fukushima, Y.: Attenuation relations of strong ground motion in Japan using site classification based on predominant period, Bulletin of the Seismological Society of America, 96(3), 898-913, https://doi.org/10.1785/0120050122, 2006.